Public-data File 85-59

ANALYSIS OF DATA FROM A TEMPORARY SEISMIC NETWORK ON UNALASKA ISLAND[1]

By

Klaus H. Jacob and Thomas M. Boyd[2]

Alaska Division of
Geological and Geophysical Surveys

November 1985

THIS REPORT HAS NOT BEEN REVIEWED FOR TECHNICAL CONTENT (EXCEPT AS NOTED IN TEXT) OR FOR CONFORMITY TO THE EDITORIAL STANDARDS OF DGGS.

794 University Avenue, Basement
Fairbanks, Alaska 99701

[1]Research funded by Alaska Division of Geological and Geophysical Surveys.
[2]Lamont-Doherty Geological Observatory of Columbia University, Palisades, New York 10964.

F I N A L   T E C H N I C A L   R E P O R T

GGSDNR-CC10-1189

ANALYSIS OF DATA FROM A TEMPORARY SEISMIC NETWORK ON UNALASKA ISLAND

Klaus H. Jacob and Thomas M. Boyd

Lamont-Doherty Geological Observatory of Columbia University

Palisades, New York 10964

Final Technical Report
GGSDNR-CC10-1189

ANALYSIS OF DATA FROM A TEMPORARY SEISMIC NETWORK ON UNALASKA ISLAND

Klaus H. Jacob and Thomas M. Boyd

Lamont-Doherty Geological Observatory of Columbia University
Palisades, NY 10964

ABSTRACT

Lamont-Doherty Geological Observatory operated a small seismic network on Unalaska Island for periods of time during the years 1980, 1981, and 1982. The cumulative effective time of monitoring the seismicity during the period of network deployment amounts to about one year, during which several hundred earthquakes were detected within the region. Of these events 148 earthquakes were locatable. They range in mangitude between mb = 1.2 and 6.1. D during the period of network operation only 18 events in this region were reported teleseismically.

The seismic hypocenters derived from the network data define beneath Unalaska Island a northwestward dipping Wadati-Benioff zone which is (during this period) restricted to depths of at most 150 km. Most of the shallow seismicity (less than 30 km deep) occurs in the portions of the Earth's crust beneath Unalaska Island closest to the Aleutian Trench, and at the contact of the fore-arc structures with the subducting Pacific plate.

No locatable seismicity was detected within 15 km of the 2036-m high Makushin Volcano and its fields of associated fumarolic activity.

However, a cluster of seismicity composed of nearly 50 events was detected more than 15 km ESE of Makushin volcano, near the Nateekin River valley. Thirteen events were locatable and weakly define a narrow, 3-km wide zone of seismicity that dips very steeply from near the surface to about 8 km depth. The true tectonic nature of this tightly clustered seismic feature is not known. P-wave first motions and P-SV amplitude ratios constrain these events to represent either left-lateral motion on a steeply dipping ENE trending fault or right lateral motion on a steeply dipping NW trending fault. The associated shallow cluster of seismicity approximately aligns with an extension of a surface lineament that cuts ESE through Makushin Volcano. On the NW flank of the volcano, this fault lineament has not been seismically active during the observation period, but apparently has controlled since about 800 y.b.p. the near-surface emplacement of magma by forming a row of recent volcanic vents extending towards Point Kadin heading into the Bering Sea. A Quarternary volcanic vent that apparently also lies on this lineament has been mapped about 18 km ESE of Makushin Volcano. It is located between the newly detected seismic cluster and the tip of Captain's Bay. Because of its location on or near the lineament, and because of its shallow depth range, we suggest that the active structure associated with the seismicity cluster is of potential importance for possible future volcanic activity at the periphery of Makushin Volcano. Also it should be thoroughly investigated for its geothermal potential at depths between 0.5 and 7.5 km.

Table of Contents

List of Tables

List of Figures

INTRODUCTION

Since 1969 Lamont-Doherty Geological Observatory has operated intermittently a single seismic station at Dutch Harbor on Amaknak off Unalaska Island. In 1980, as part of NOAA-BLM's Outer Continental Shelf Environmental Assessment Program (OCSEAP) which had the mission to evaluate seismic and volcanic hazards, Lamont enlarged its seismic monitoring program to a five-station seismic network. Thus, for the first time it became possible to locate earthquakes more accurately in the vicinity of Unalaska than is possible by teleseismic means. The sudden termination of OCSEAP in 1983 forced the dismanteling of the network and left most of the collected network data uninterpreted. At the same time the State of Alaska through its Power Authority and Division of Geological and Geophysical Surveys (DGGS) became interested in assessing the geothermal power potential of Makushin Volcano and associated fumarolic fields for providing an economic local energy source to the expanding industrial base at Unalaska and Dutch Harbor and its communities. Since microearthquake data have been repeatedly proven helpful in assessing productive structures in geothermal regions, DGGS commissioned a study to process and analyze the existing network data to reveal any hidden or buried active faults, especially near geothermal prospects, on Unalaska Island. The following report is the result of this analysis effort concentrating on the network data only. A corollary paper has been prepared focussing mostly on the teleseismic data and historic seismicity of the large Unalaska region (Boyd and Jacob, 1985). That second paper reviews the seismic potential of the "Unalaska Seismic Gap". This gap may not have ruptured recently in a major earthquake while other segments of the plate boundary to the east and west may have done so during the great earthquakes of 1946 and 1957, respectively. The seismic potential for a future great earthquake at the Unalaska portion of the eastern Aleutian arc has been previously discussed extensively in the literature (Sykes et al., 1981; House et al., 1981; Jacob, 1983).

SEISMIC NETWORK

Starting in 1978 an effort was made to improve seismic monitoring from the single station operated in Dutch Harbor, to a network of telemetered stations. The intent was to locate seismic events rather than only registering their occurrence in time. A functional network with central automatic event detection and magnetic-tape analog-recording did not become operative, however, until 1980. The new recording system using a common, accurate time base, improved the relative timing between stations (to better than .01 seconds) to enable tectonically meaningful locations of the seismicity. The limited aperture of the five-station network (Figure 1 and Table 1) measures, however, only about 55 km along strike of the arc, and barely 30 km normal to the arc. This spatial limitation therefore restricts the reliable hypocenter locations to the immediate vicinity of Unalaska Island.

Only two stations were located on Unalaska Island proper (Figure 1): USR at the upper headwaters of Shaisnikof River, and MAK at the western end of Makushin Valley enroaching on the ridge that connects Makushin volcano with Tabletop Mountain north of Makushin Valley. The other two remote stations were SDK on Sedanka Island just off SE

Unalaska Island, and AKA near the western slopes of Akutan Island. The radio repeater site BLH, Ballyhoo, and the central recording site DUT, Dutch Harbor, are located on Amaknak, an islet in Unalaska Bay.

All remote stations consisted of single-component vertical 1-Hz geophones (Geospace HS10) with amplifier - VCOs. Their output FM audio carrier was modulated onto an VHF radio-carrier whose waves were beamed by yagi antennas to the radio relay site, BLH, atop Mount Ballyhoo. From there, the signals were retransmitted on a single FM carrier to the central station DUT at Dutch Harbor. The only exception to this relay scheme is station MAK whose radio signal could be beamed with direct line of sight to DUT and received there.

At the central recording site DUT, a 3-component set of 1-Hz Baby-Benioff seismometers was operated and their amplified signals were FM-modulated and mixed for multiplexed FM recording with the FM signals from the remote stations on a TEAC 4-trac tape-recorder. That recorder was operated only discontinuously when triggered by an event. The trigger system consisted of analog STA/LTA ratio detection of the levels of the demodulated incoming seismic signals and search for coincidence for high STA/LTA ratios at more than one station. If such a coincidence occurred an event was declared. Event declaration prompts the transfer of the FM seismic signals from a second, continuously recording TEAC tape recorder to the event-only-recording TEAC unit. The continuous-recording unit had been modified to operate on an endless tapeloop. This modification allows to retroactively recover seismic signals at least some 20 seconds prior to event declaration. This pre-event recovery ensures coverage of first arrivals, that are too faint to declare an event by themselves.

In addition to the analog recording of distinct events, Helicorder recordings produced a continuous visible writing of the seismic signals of at least one network station to check on background microseisms, frequency of events in time, and on the reliability of the event trigger system. A GEOS satellite receiver clock inserted a code of Universal Time (UCT) into the analog datastream, with an accuracy of better than one thousandst of a second.

The analog tapes were shipped to Lamont. There the analog event-detected signals were semi-automatically digitized and transferred to computer-compatible tape and then processed on Lamont's seismology computer (PDP-11/70). P- and, where applicable, S-arrival times were picked interactively from traces on a CRT screen, together with maximum body-wave amplitudes for magnitudes determination. The P- and S-phase data are fed into the HYPOINVERSE computer routine (Klein, 1978), using the velocity structure of Table 2, that is also used at Lamont for the Shumagin Islands seismic network (Reyners and Coles, 1982). A sample record of an event in the Unalaska array with phase picks is shown in Figure 2, and a sample output from the location routine HYPOINVERSE for an event is shown in Figure 3.

SEISMICITY

Regional Pattern. A total of 148 earthquakes were locatable from the gathered network data. They are shown in map view in Figure 4, in section along a profile AB striking normal to the arc in Figure 5, and are tabulated in Table A1 (see Appendix 1). The following main patterns of this seismicity emerge:

The shallow seismicity, taken here as that with depths less than 50 km, is most prominently distributed at a band coinciding with, and paralleling, the 1000-m bathymetric contour that straddles the islands of Unimak, Unalaska, and Umnak (Figure 4). Only on Unalaska does this activity encroach onto the chain of islands itself. There it coincides with the northeasternmost down-dip extent of the 1957 aftershock zone and inferred rupture zone of this major event (M_w = 9.1). East of longitude 165°W and west of 167°W, the shallow seismicity extends towards the trench, in approximate accordance with the rupture zones of the 1946 and 1957 great earthquakes, respectively, outlined in Figure 4. A single event near the southern terminus of profile AB, seaward of the trench, is probably a normal-faulting event associated with the flexure of the Pacific plate forming the outer rise.

Quiescent Zone. There is a conspicuous paucity of shallow earthquakes between the 1000-m bathymetric contour and the Aleutian Trench near the Unalaska Basin and some 100 km to the NE of it, coinciding closely with what has been termed the Unalaska Seismic Gap based on historic, tsunami, and instrumental teleseismic data. The relationship of the local and teleseismic/historic patterns of seismicity associated with the Unalaska Seismic Gap are discussed in detail by Boyd and Jacob (1985).

Wadati-Benioff Zone. The intermediate-depth seismicity (>50km deep) is clearly visible in cross section (Figure 5) to form a reasonably well defined Wadati-Benioff zone that presumably outlines the path of descent of the subducting Pacific lithosphere to depths of at least 150 km. The actual maximum seismogenic depth in the descending slab is probably close to 250 km as inferred from the deepest events in adjacent segments (Reyners and Coles, 1982) and from teleseismic data (Jacob et al., 1977; Davies and House, 1979). But during the limited period of observation no events deeper than about 150 km were located. The dip of the shallow portion of the plate interface in the subduction zone is inferred to be about 12 degrees between the trench and a depth of 30 km, below which the dip of the Wadati-Benioff zone increases to about 48 degrees (Boyd and Jacob [1985], and Figure 5).

There is a prominent absence of earthquakes in the Wadati-Benioff zone at depths from about 90 to 130 km, directly beneath the line of active volcanoes. A zone of reduced activity in the Benioff zone is often observed beneath volcanic arcs worldwide. It may be an inherent property of seismicity in most subducting slabs at depths of about 100 km. The cause for this reduced seismicity is not known but one can speculate that it is related to the mobilization of volatiles from the upper surface of the descending slab. The volatiles may in turn give rise to the partial melt in the overlying mantle. Upwelling of the magmas then forms the volcanic arc. The volcanic arc (see cross section of Figure 5) is located above an imaginary depth contour of the upper envelop of the Benioff zone where it is approximately 110 km deep.

A number of scattered events are located at about 50 km depth beneath the volcanic line. They are either mislocated events due to refracted arrivals from the slab since they belong mostly to events near the periphery of the network; or the events would be highly unusual since they are located in what elsewhere is commonly known as the "aseismic wedge". Its leading edge towards the trench demarcates the "aseismic front", another globally observed feature of subduction zones. The aseismic front presumably defines the locus of a change in rheology at the plate interface. Updip from the aseismic front the deformation at the plate interface is elastic-brittle and seismogenic, while downdip from it deformation appears to occur by aseismic creep implying that all deeper observed seismicity occurs within the slab rather than at its interface with the yielding overlying mantle. From the section in Figure 5 we infer that the depth at which this transition in the rheology of the plate interface occurs beneath Unalaska Island is about 30 km.

Local Patterns. To show more closely any potential relationship between shallow seismicity and geologically mapped surface or near-surface features we superimpose the located earthquakes onto a simplified geologic map of Unalaska Island (Figure 6). With the exception of a tight cluster of seismicity about 18 km ESE of the summit of Makushin Volcano, virtually all remaining shallow seismicity is near the southern, mountainous, and coastal portions of the Island. A distinct linear cluster of events is located beneath the western beach line of Usof Bay which forms the most prominent fjord-like incision into the Shaler Pluton. While this fjord is almost certainly carved by ice during the last local glaciation, its location may well be tectonically controlled. However, no mapped fault is at present known to be associated with this seismic and morphologic lineament. Nor were we able to derive a fault plane solution for the seismic cluster because of poor azimuthal coverage on the focal sphere by the sparse network.

A mere four events are located on the SW limb of Unalaska Island that sretches for about 60 km from Shaler Pluton to Konets Head facing Umnak Passage. Given the uncertainties in the locations far outside the network, these earthquakes could be loosely associated with a mapped linear feature more than 20 km long (Plate 77, Drewes et al., 1961);

this lineament also shows prominently on a SLAR map of the Island (Unalaska, 1981). It strikes WSW as a morphologic feature within the Unalaska Formation whose rocks make up the spine of this portion of Unalaska. Except for scattered events that plot in mapview on the exposures of Shaler Pluton and Captains Bay Pluton, the remainder of Unalaska Island is virtually devoid of shallow crustal seismicity during the period of observation.

Seismic Quiescence of Makushin Volcano and Fumarolic Fields. The peninsular protrusion of Unalaska Island extending northwestward into the Bering Sea is dominated by the 2036-m high, glaciated Makushin Volcano. The NE half of this portion of Unalaska is made up of unaltered recent volcanic rocks, while its remainder is composed of rocks of the Unalaska Formation of upper Oligocene to middle Miocene age. This entire area NE of the land narrows that connect Captians with Portage Bay is - during the period of observation with one distinct exception - completely free of shallow crustal earthquakes (Figure 6). This is remarkable, since the vicinity of Makushin Volcano and related secondary volcanic centers is known to be traversed by Holocene faults, some with scarps as high as 5 meters (Reeder, 1984). Many of the subsidiary cones and the fumarolic fields seem to be aligned with some of the faults, presumably using these zones of weakness as a path of ascent of magma or thermal waters and steam. The apparent seismic quiescence could be either a temporary one, or may signify that any strains in the vicinity of the active volcanic structure are released aseismically because of the high temperatures even at near-surface depths.

Cluster of Seismicity near Nateekin River Valley. The only seismically active feature detected in the NE portion of Unalaska Island is a cluster of small earthquakes located near 53° 50'N and 166° 42' W (Insert to Figure 6). It occurred as a swarm over a relatively short period of time, from August 6 through 11 of 1981. The cluster of events is located about 17 km ESE of the summit of Makushin Volcano, approximately on the ESE extension of a system of steeply dipping dip-slip (probably normal) faults that strike about N70 W; they start in the NW at Point Kadin, cut through the NE flank of the Makushin summit caldera rim, and proceed ESE as a set of two parallel faults towards Captians Bay Pluton (Reeder, 1984). The northeastern one of the two faults appears to have provided the locus of ascent of magma that forms a Quarternary volcanic vent on the southern valley slopes of the Nateekin River, about 4 km east of the SW tip of Captains Bay. The isolated vent is the most distant vent from Makushin summit that appears to be related to the ongoing phase of volcanism on Unalaska Island as presently mapped.

Figure 7 shows the cluster of seismicity in more detail both in map view and in two cross sections, AA' striking SE and BB' striking NW. Comparison of the two sections shows a tighter clustering of the 13 locatable hypocenters apparently forming a steeply SW-dipping "fault" on section BB'. The hypocenters when projected on section AA' appear to not fall as readily on a single plane, although the distribution of hypocenters does not clearly discount a SE dipping structure. The composite focal mechanism derived from first motion data and P-SV amplitude ratios (Appendis B; Figures B1 and B2) of all the well located events in the swarm indicate that the active fault is either NE or SE dipping. Since cross-section BB' clearly discounts the possibility of rupture along a NE dipping fault plane, left-lateral slip occurring, on a SE dipping plane is more consistent with cross-section AA' and the composite focal mechanism.

Only 13 events of this swarm-like cluster were locatable from the event-triggered tape-recorded array data. A systematic screening of the Helicorder/continuously-monitored recordings for station USR showed that a total of 48 events with virtually identical S-P times and signal characters may have originated from the same general source or active structure. At least the 13 locatable events are confined to depths from at least .15 to 7.5 km.

DISCUSSION

In the context of assessing the potential for geothermal energy resources on Unalask Island, the cluster of seismicity near the Nateekin River Valley is the only detected seismogenic feature of interest, since the remaining vicinity of Makushin Volcano behaved aseismically. Several characteristics of this seismic cluster are unusual. Their geometric aspect ratio of width (3 km) to depth (8 km) of the activated source area make for a very skinny, almost tinsel- or pencil-like structure. If motion on an active fault structure occurs seismically, it is difficult to understand how it can be confined to a strip so narrow; or if slip is not confined to the 3-km wide strip, why would it occur seismically only at the narrow strip, and aseismically beyond it? The best fit to the available data as described above is compatible with a strike-slip solution implying left-lateral slip on a NE-striking plane. This fault-plane solution is however, is not fully compatible with the system of mapped ESE-striking normal faults that stretch from Point

Kadin through Makushin caldera and the seismic cluster to the isolated volcanic event W of Captians Bay.

If the mapped ESE striking normal faults exist and actively participate in a rifting or opening normal to their strike, and if the confined cluster is related to this mode of regional rifting deformation, then the seismic cluster would be most readily explained as activity on a right-stepping offset between two rift zones, much like on a ridge-ridge transform fault that is active only between the two offset ridges, but not beyond them. In that case the active transform would strike NNE, dip more or less vertically, and have a left-lateral sense of strikeslip motion, which is compatible with the solution shown in Figure B1 (Appendix B); and less compatible with the optimal event alignment to a NE-striking, SW-dipping planar feature as inferred from Figure 7 and discussed earlier. Despite these inconsistencies we offer this model depicted in a schematic sketch (Figure 8), to explain the peculiarly narrow, pencil-like geometry of the cluster that is probably its best determined property. Neither the focal mechanism nor the dip and strike of a plane fitted to the hypocenters are as equally well constrained as the general shape of the cluster.

The occurrence of the events in a single episodic swarm and the small magnitudes ranging from mb = 1 to 2.6, are reminiscent of seismic events associated with volcanic episodes; however the b-value of 1.1+0.4 (see Appendix C) is not. Volcanic earthquakes often have b-values exceeding 2.0 (e.g., Minakami, 1960; Minakami et al. 1969), while values near 1.0 - as observed here - are more typical for tectonic event sequences. To reconcile these observations with the model depicted in Figure 8, one could speculate about a volcanically driven, aseismic extension of the ESE striking rift- or normal-faulting system, which causes seismic (tectonic) events on the associated right-stepping transform fault segment. This scenario, far from provable by the present data, would be compatible both with the volcanic temporal but tectonic b-value characteristics of this event sequence.

The implications of the broader patterns of seismicity at and around Unalaska Island and their possible relations to the potential for a future great earthquake in the Unalaska Seismic Gap are discussed in Boyd and Jacob (1985). Some details about the range of magnitudes detected by the network, completeness of detection, an magnitude - frequency of occurrene relationships are deferred to the Appendix C of this report.

CONCLUSIONS

During a three-year period from 1980 to 1982 a temporary seismic network was operated in the vicinity of Unalaska Island. During monitoring times cumulatively amounting to about one year, several hundred events were detected and recorded, of which about 150 events were located. By-and-large, the hypocenter distribution mimics the teleseismic patterns with a well defined Wadati-Benioff zone, shallow seismicity associated with the plate interface of the main thrust zone of the subduction complex. This similarity also extends to the region of the previously defined "Unalaska Seismic Gap" that is relatively quiescent. Some shallow seismicity is scattered throughout the southern, trenchward portions of the island, that are made up of the Unalaska Formation (of upper Oligocene to middle Miocene altered rocks) and of the 11 to 13 million year old plutons, most prominent amongst them the Shaler and Captains Bay Pluton. The region surrounding Makushin Volcano and other volcanic cones and vents on northern Unalaska which are largely made of Quarternary to Recent volcanic rocks, is virtually aseismic despite the evidence of Holocene faulting. A single cluster of some 50 small seismic events was detected and 13 events located to form a pencil-like active structure near a set of ESE-trending (normal ?) faults and a nearby isolated Quarternary volcanic vent a few kilometers west of Captains Bay. The exact tectonic nature of this event sequence could not be deduced from the limited data; its location and geometry, however, make it - if not likely - so at least compatible to be associated with a system of ESE trending faults. Elsewhere - closer to the summit of Makushin - and at earlier times, the mapped faults have provided avenues for magma ascent and hydrothermal circulation and provide at present some of the conduits for active fumaroles on the slopes of Makushin and secondary volcanic cones. Because of these associations we suggest that the cluster of seismicity detected during this study may be a potential target for future geothermal studies. In other geothermal prospects of the world shallow seismicity detected faults have been proven to be excellent geothermal producers. For instance during a microearthquake survey of the Ahuachapan geothermal field in El Salvador, Ward and Jacob (1971) identified a seismic fault at depth whose surface projection intersected a known field of active fumaroles; subsequent drilling into this buried fault yielded several productive steam wells, still used for electric power generation more than a decade later. While no fumaroles are known to be active in the immediate vicinity of the detected cluster of seismicity near the to Dutch Harbor/Unalaska and its lower elevation make it a logistically more feasible target than some less accessible sites on the slopes of Makushin Volcano. Clearly more geophysical work (for instance resistivity surveys and heatflow surveys) would be required in addition to more focussed microearthquake surveys, before a more definitive assessment of this feature for geothermal purposes can be given.

APPENDICES

Acknowledgements. This work was supported by the Division of Geological and Geophysical Surveys (DGGS) of the Department of Natural Resources, State of Alaska. We thank Dr. John Reeder for productive cooperation during the study, in the field, an for providing preprints of papers prior to publication. The seismic network was initially installed with funds from OCSEAP whose assistance we gratefully acknowledge. Many individuals from Lamont (formerly or now) helped in the field and in the early stages of data preparation, amongst them Egill Hauksson, Laszlo Skinta, John Davies, and Mary-Ann Luckman, Rosemarie Bongiorno typed the manuscript and Kazuko Nagao prepared some of the drawings. Lamont-Doherty Geological Observatory Contribution Number 0000.

REFERENCES

Boyd, T. and K. Jacob, 1984. Seismicity of the Unalaska region, Alaska, in preparation.

Davies, J. and L. House, 1979. Aleutian subduction zone seismicity, volcano-trench separation and their relation to great thrust-type earthquakes, J. Geophys. Res., 84, 4583-4591.

Drewes, H., G. Fraser, G. Snyder, and H. Barnett, 1961. Geology of Unalaska Island and adjacent insular shelf, Aleutian Islands, Alaska, Geological Survey Bulletin 1028-S, 583-676.

House, L., L. Sykes, J. Davies and K. Jacob, 1981. Identification of a possible seismic gap near Unalaska Island, Eastern Aleutians, Alaska, in Earthquake Prediction, An International Review, Maurice Ewing Series, 4, D.W. Simpson and P.G. Richards (eds), AGU, Washington D.C, 81-92.

Jacob, K., 1983. Estimates of long-term probabilities for future great earthquakes in the Aleutians. Geophys. Res., Letters, 11, 295-298.

Jacob, K., K. Nukamura and J. Davies, 1977. Trench-volcano gap along the Alaskan-Aleutian arc: Facts, and speculations on the role of terrigeneous sediments, in Island Arcs, Deep Sea Trenchs, and Buck-Arc Basins, Maurice Ewing Ser., vol. 1, M. Talwani and W.C. Pitman III (eds.), AGU, Washington, D.C. 243-258.

Klein, 1978. Hypocenter location program HYPOINVERSE, Part 1: Users guide to versions 1, 2, 3, and 4: Part 2: Source listings and notes, U.S. Geol. Surv. Open-File Rpt. 78-294, 114 pp.

Reeder, J., 1984. Fault and volcanic dike orientations for the Makushin Volcano region of the Aleutian Arc, Royal Society of New Zealand Bulletin, in press.

Reyners, M. and N. Coles, 1982. Fine structure of the dipping seismic zone and subduction mechanics in the Shumagin Islands, Alaska, J. Geophys. Res., 87, 356-366.

Sykes, L., J. Kisslinger, L. House, J. Davies, and K. Jacob,d 1981. Rupture zones and repeat times of great eartqhuakes along the Alaska-aleutian arc, 1784-1980, in Earthquake Prediction, An International Revies, Maurice Ewing Series, 4, D.W. Simpson and P.G. Richards (eds), AGU, Washington D.C., 73-80.

Unalaska, 1981. Synthetic-aperture radar imagery near range X-band, Northwest look, experimental edition, Alaskan Geology Branch, 531 66-C1-RA-250-XO.

Ward, P. and K. Jacob, 1971. Microearthquakes in the Ahuachapan Geothermal Field, El Salvador, Central America, Science, 173, 328-330.

Minakami, T., 1960. Fundamental research for predicting volcanic eruptions (I) - Earthquakes and crustal deformations originating from volcanic activities. Bull. Earthquake Res. Inst., 38, 497-544.

Minakami, T., S. Hiruga, T. Miyazaki, and S. Utibori, 1969. Fundamental research for predicting volcanic eruptions (Part 2). Bull. Earthquake Res. Inst., 47, 843-950.

Habermann, R., 1983. Teleseismic detection in the Aleutian Island Arc, J. Geophys. Res., 88, 5056-5064.

Table 1
Unalaska Network Station Characteristics

Station	Location		Operational Date	Seismometer
DUT	53° 53.9' *N*	166° 32.2' *W*	8/79	3B
AKA	54° 05.8' *N*	166° 01.9' *W*	8/79	N
MAK	53° 55.4' *N*	166° 43.8' *W*	7/80	N
SDK	53° 50.3' *N*	166° 09.4' *W*	7/80	N
USR	53° 46.0' *N*	166° 41.8' *W*	6/81	N

N=Single short period seismometer (Norsar HS-10)
3B=Orthogonal set of short period seismometers (Baby Benioffs)

Table 2
Flat-Layered P-Velocity Model for the Unalaska Island Array

P-Wave Velocity of Layer (km/sec)	Depth to Top of Layer (km)
3.44	0.00
5.56	1.79
6.06	3.65
6.72	10.18
7.61	22.63
7.90	38.51
8.26	90.19

A ratio of P-wave velocity to S-wave velocity of 1.73 was adopted for all layers.

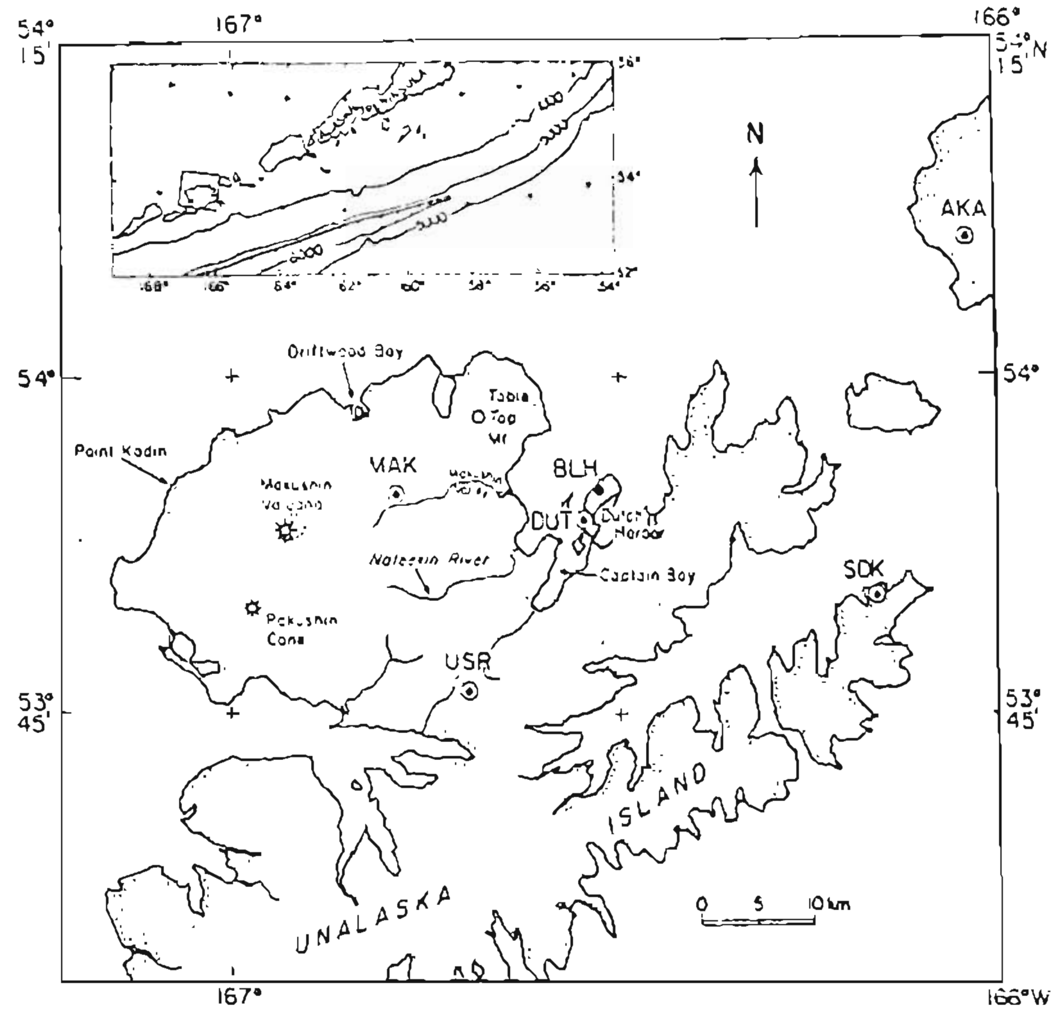

Figure 1. Unalaska Island Array, Eastern Aleutians, and geographic place-name positions referenced in the text. The array consisted of four remote stations, MAK, USR, SDK, and AKA with short-period, vertical seismometers. At the central recording site, DUT, a three component set of seismometers was operated. BLH is a repeater station for signals that are telemetered from the remote station and recorded at the central site.

Figure 2. Sample seismograms for an event occurring on August 6, 1981 from stations DUT and SDK. The distance between tickmarks is 1 second. Also shown are the P and S arrival times picked by the data analyst.

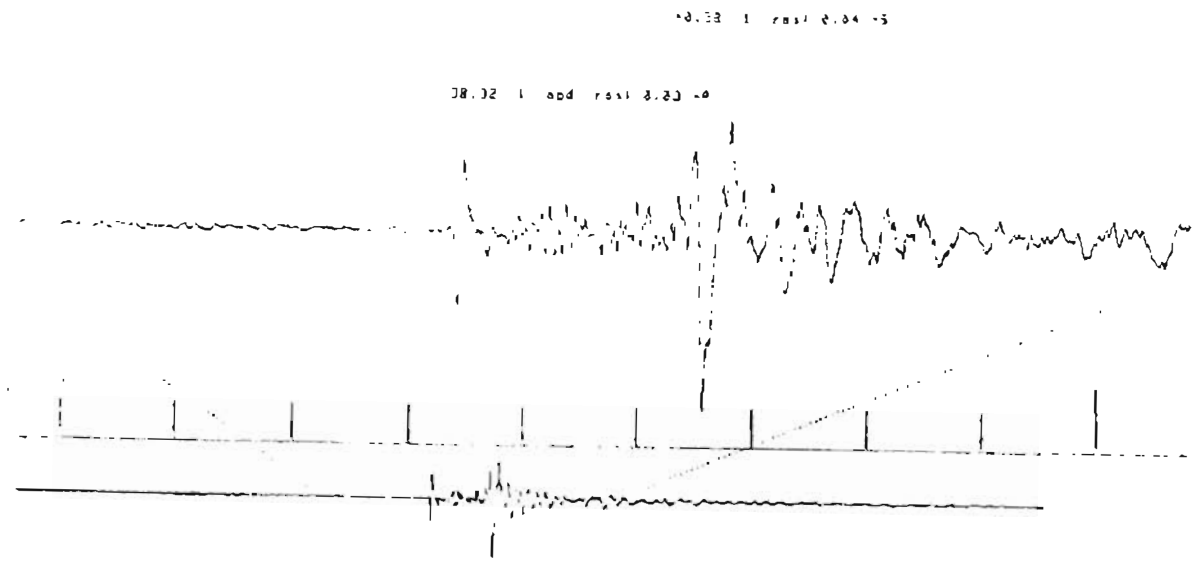

Station: aska 35.11 -- 55.11 - - - - 1981/08/06 14:53:24.00 59

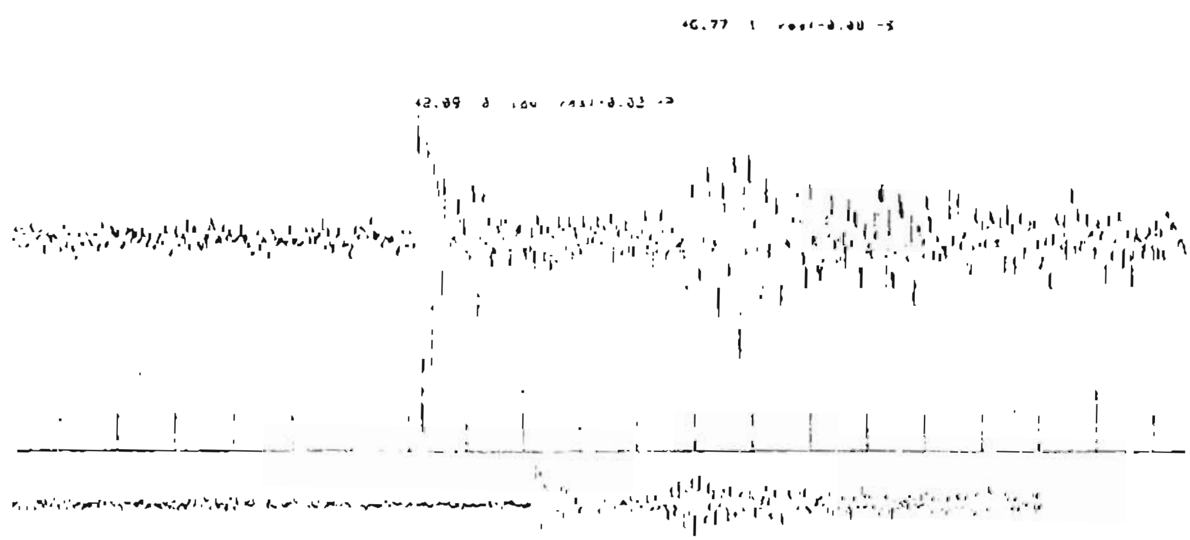

Figure 3. Standard locational output from HYPOINVERSE (top portion of figure) and a data display program written by C. Nicholson (lower portion of figure). The HYPOINVERSE solution contains; hypocenter parameters and error estimates, and P and S arrival time residuals, estimated takeoff angles, distances, and azumuths for each station. The display output includes a Wadati diagram (upper-left), a Riznichenko diagram (lower-left), a map with the estimated epicenter (upper-right), and a upper hemisphere focal mechanism plot (lower-right).

```
the 810806.145924o file is:

l  6 aug 81, 14159  event no.   1

------------------------------------------------------------------------------------------
 yr mo da   origin     lat n     lon w    depth  rms   erh   erz gap xmag fmag
 81- 8- 6 1459 35.65 53 50.22 166 42.02  4.60  .03   .15  1.26 149  2.4

 rmswt dmin itr nfm nwr nws remk q sqd
   .03  7.8   3   4   8   4  ad  b a c

  sta dist azm  an p/s w   sec*cor (tobs -tcal -dly  +res) wt  xmg fmg r info
usrz   7.8 177 106 ipd    37.55  .00  1.30  1.28  .00   .02 1.28          .465
                   s  1 38.86  .00  3.21  3.25  .00  -.04  .96           .694
makz  10.3 326 100 ipd    37.92  .00  2.27  2.27  .00   .00 1.28          .008
                   s  3 39.48  .00  3.83  3.93  .00  -.09  .32           .123
dusz  12.7  57  97 epd 1 38.32  .00  2.67  2.66  .00   .01  .96 2.3      .163
                   s  1 40.29  .00  4.63  4.60  .00   .03  .96           .773
sdkz  35.7  89  91 iou    42.09  .00  6.44  6.45  .00  -.01 1.28 2.6      .582
                   s  1 46.77  .00 11.12 11.16  .00  -.04  .96           .388

the trial solution was:
8108061459356153 5038166 4230  45223  7204  8   325182 177109 5  31 0ad   14 4 3  32 176 411.73

810806.145924p - the original pickfile from ping
810806.145924c - the condensed output pickfile with converted amplitudes
810806.145924o - the legible version of 810806.145924c
810806.1459247 - the solution in hypo71 format
810806.145924h - the solution in hypoinverse format
chantjun81 is the gain file used
this run was executed on: Thu Oct 13 14:04:44 EDT 1983
mkdir: cannot make directory 810806.145924L
```

```
Yr Mo Dy  Origin     Lat N    Lon W   Depth Mag  RMS  Erh   Erz  Nsta Gap Dmin Nwr Nws Up/Us No.
81- 8- 6 1459 35.65 53 50.22 166 42.02  4.60 2.4 0.03 0.15  1.26   4  149   8   8   4  1.73  1
```

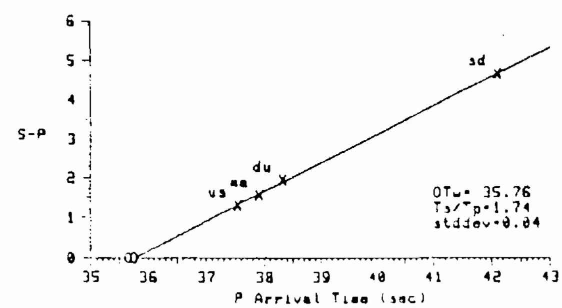

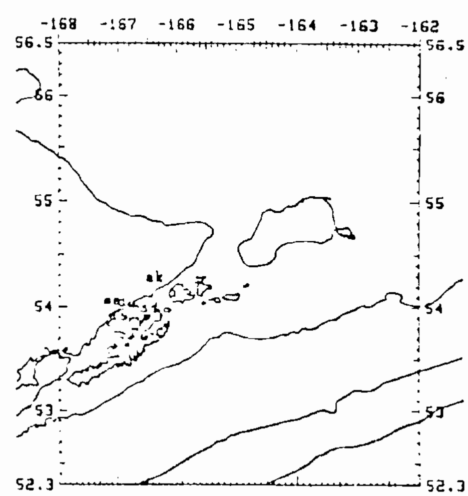

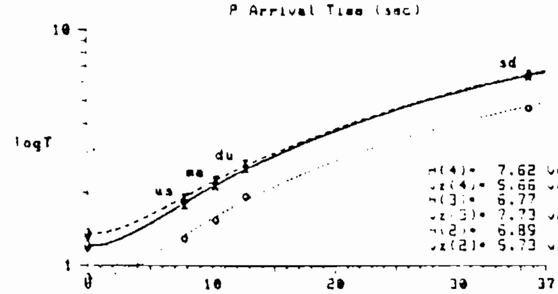


```
Sta Dist Azi Ain Prmk  Psec   Tobs Pres  Pwt   Srmk  Ssec   Tobs Sres  Swt  Vp   Vs  Vp/Vs
us   7.8 177 106 ipd0 37.55  1.30 0.02 1.27   s 1 38.86  3.21-0.04 0.95 4.77 2.82  1.69
ma  10.3 326 100 ipd0 37.92  2.27 0.    1.27   s 3 39.48  3.83-0.09 0.31 4.97 2.95  1.69
du  12.7  57  97 epd1 38.32  2.67 0.01 0.95   s 1 40.29  4.63 0.03 0.95 5.06 2.92  1.73
sd  35.7  89  91 ipu0 42.09  6.44-0.01 1.27   s 1 46.77 11.12-0.04 0.95 5.59 3.24  1.73

real       50.0
user       15.1
sys         5.6
```

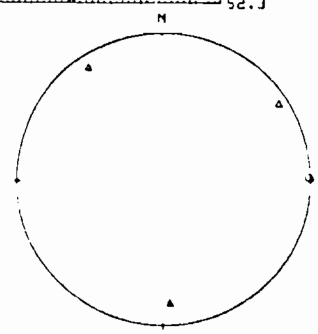

Figure 4. Seismicity located by the Unalaska seismic network. Bathymetry is in meters and hatched zone represents the trench. Aftershock zones of the great 1957 and 1946 earthquakes are represented by the dot-dashed and the dashed lines prespectively. Circles are events whose calculated focal depths are less than 50 cm while squares are events deeper than 50 km.

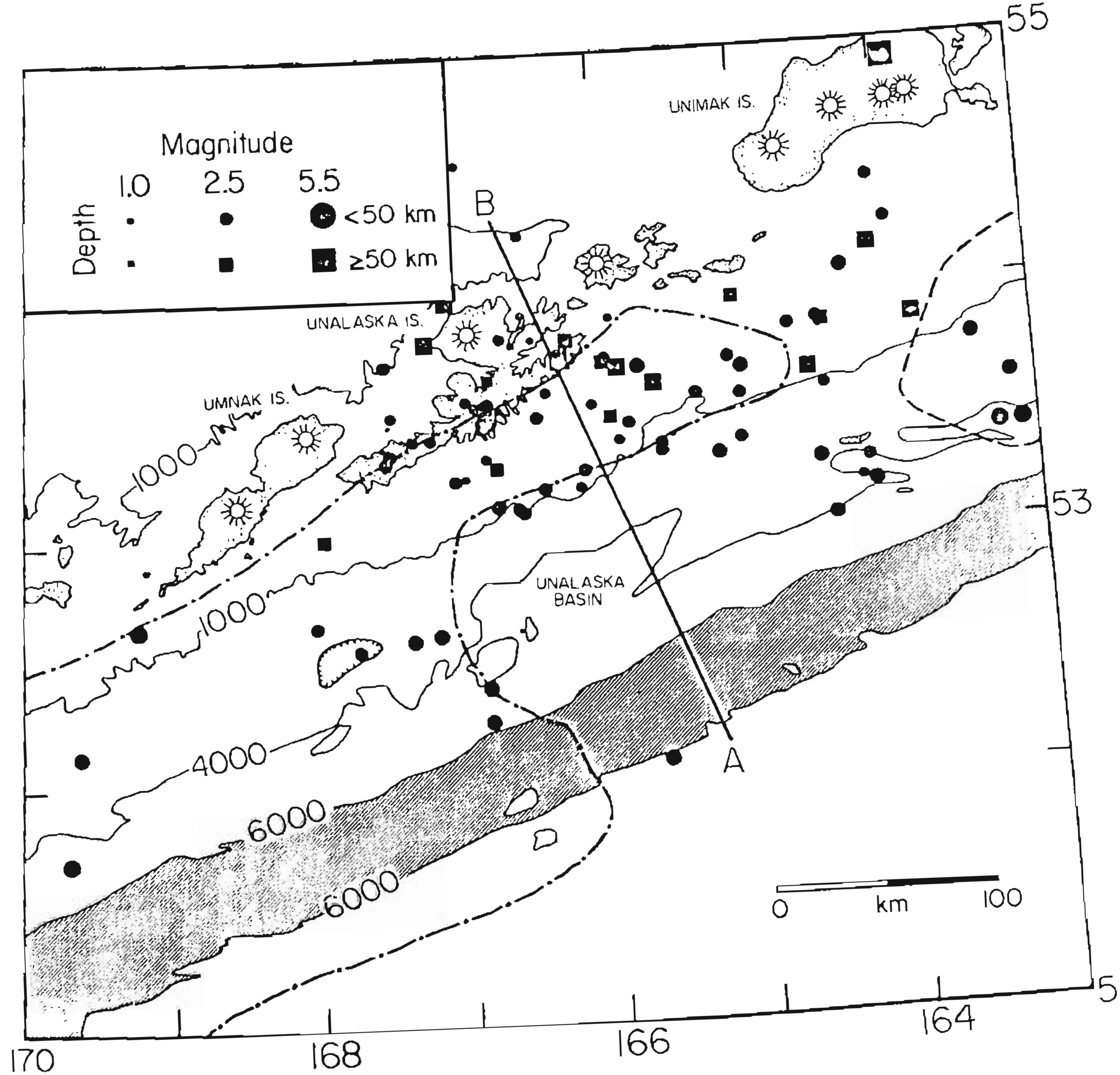
Magnitude
1.0
2.5
5.5
Depth
<50 km
≥50 km
UNIMAK IS.
UNALASKA IS.
UMNAK IS.
UNALASKA BASIN
B
A
1000
1000
4000
6000
6000
0
km
100
55
53
51
170
168
166
164

Figure 5. Vertical cross-section of the seismicity in Figure 4 through line AB. Width of cross-section is 150 km on either side of AB. Trench position is designated by a T on the top horizontal axis while the bar above this axes represents the projection of the network dimensions.

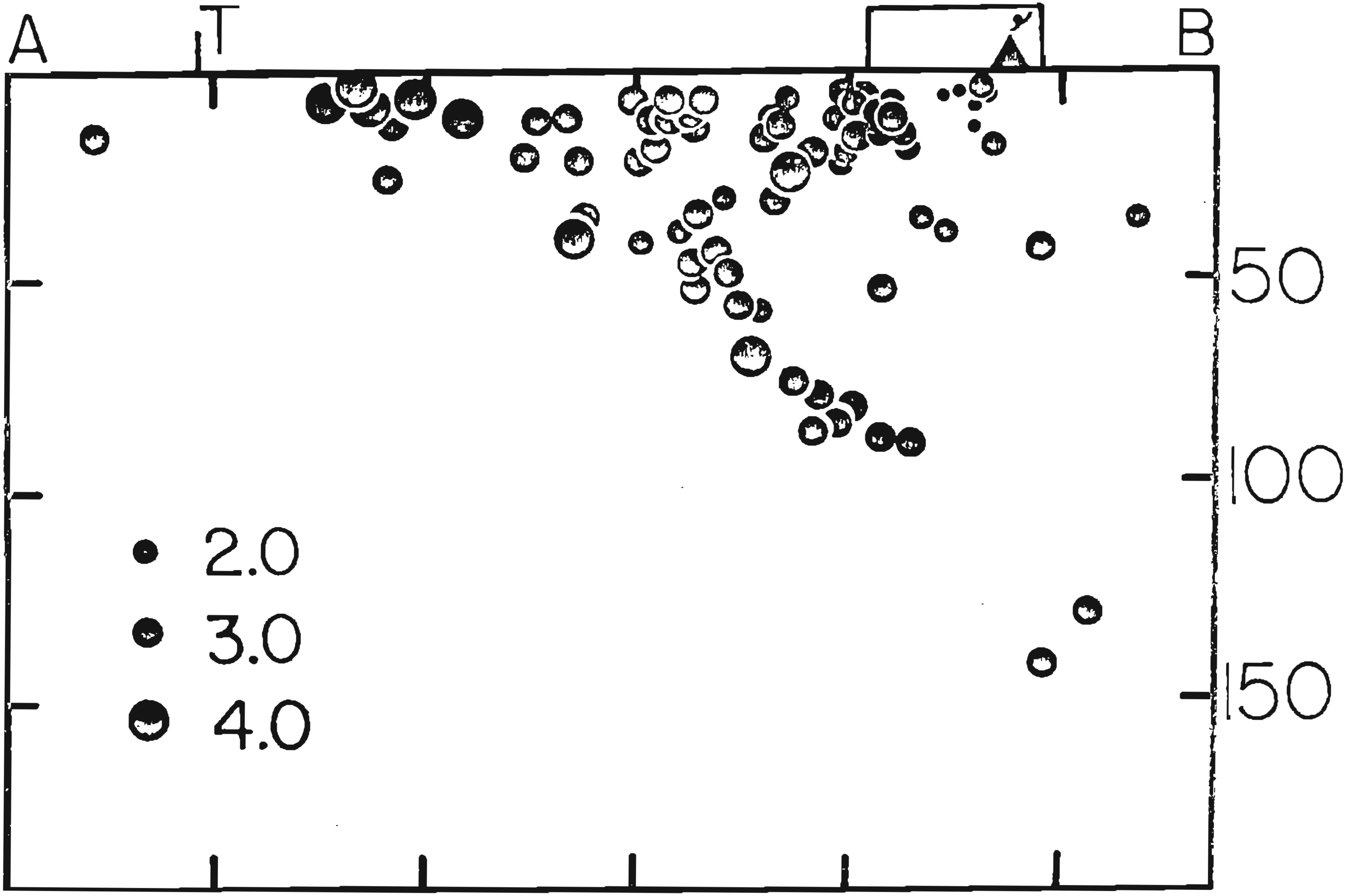

A
T
B
50
100
150
2.0
3.0
4.0

Figure 6. Geologic and seismic map of Unalaska Island. Circles are events shallower than 35 km while squares are deeper than 35 km. Open triangles show the position of four stations of the Unalaska seismic array. The unmarked areas of the map are where the Unalaska formation outcrops, the dotted areas are outcrops of platonic rocks, and the stippled areas are the recent volcanics. Faults are denoted by dashed lines. All the faults shown are high-angle normal faults. Geology is from Drewes et al. (1961).

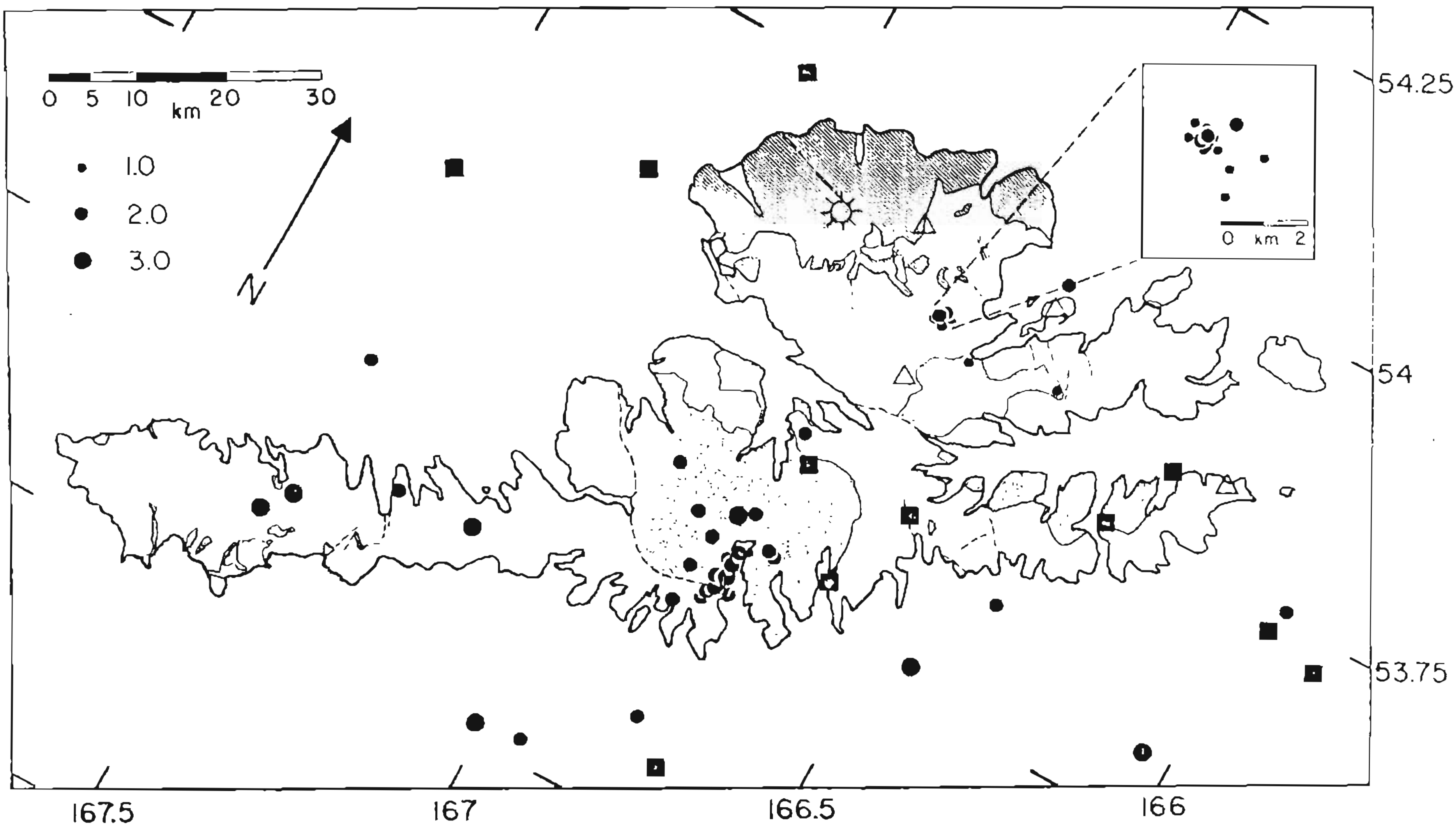

0 5 10 km 20 30
N
1.0
2.0
3.0
0 km 2
54.25
54
53.75
167.5
167
166.5
166

Figure 7. Epicentral distribution of the Nateekin River seismic cluster. Lines AA' and BB' denote lines through which cross sections of the seismicity have been projected. In cross-section, open symbols indicate events with poor depth control.

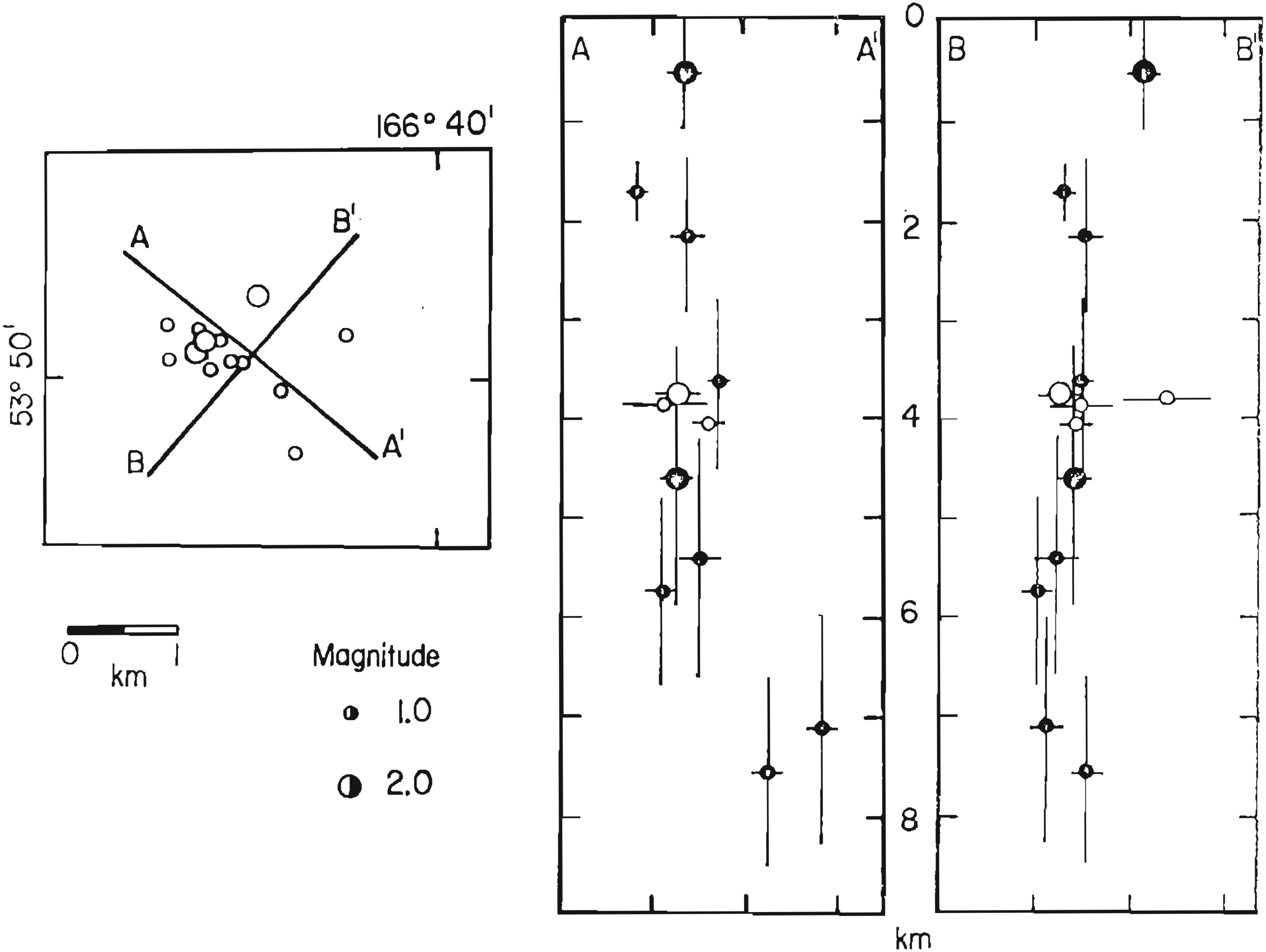
166° 40'
53° 50'
A
A'
B
B'
0
km
1
Magnitude
1.0
2.0
0
2
4
6
8
km

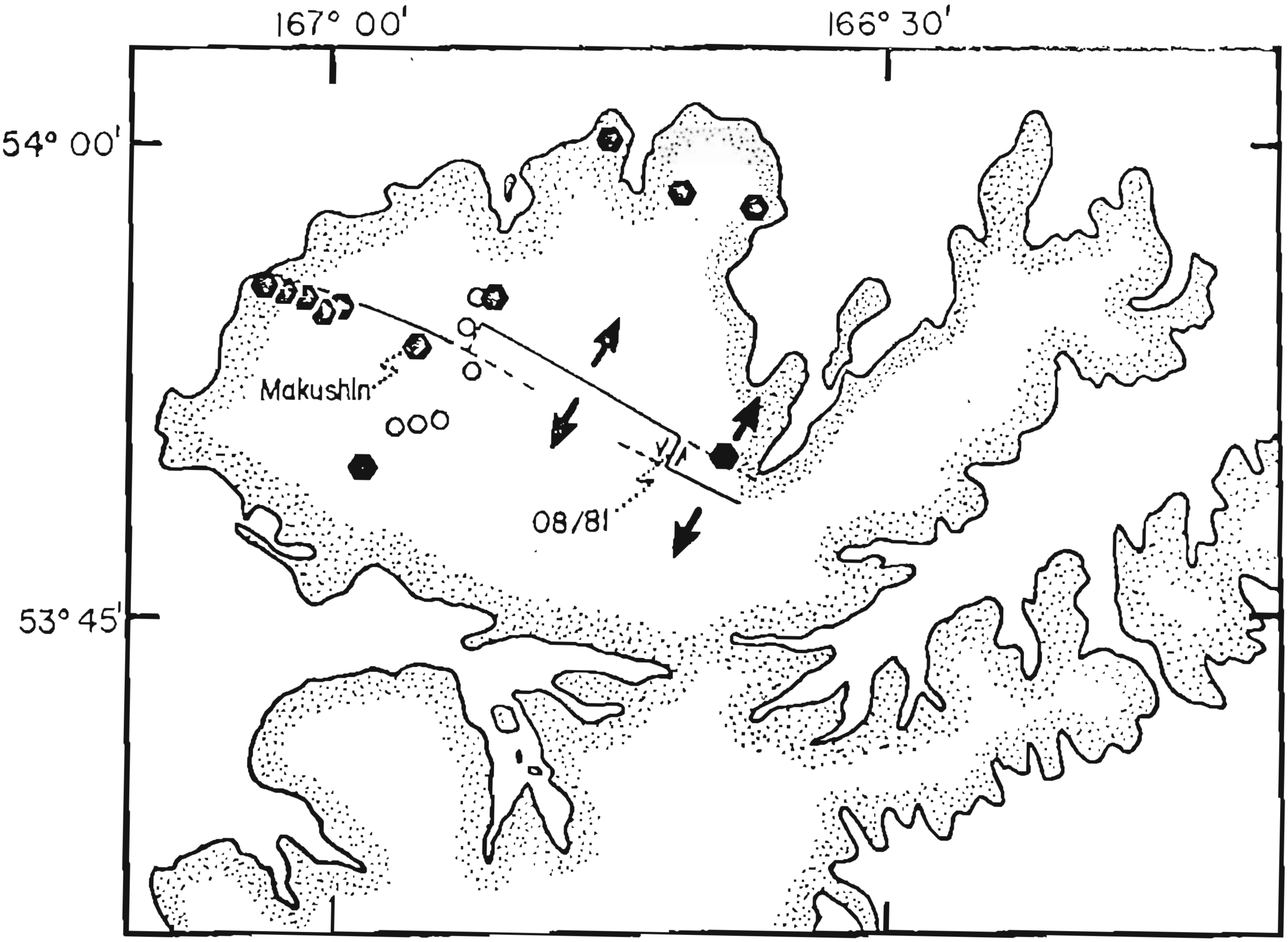

Figure 8. Interpretation of the Nateekin River seismic cluster depicting the suggested relationship between the ESE trending, aseismic normal faults, secondary volcanic vents, Makushin summit caldera, and the seismic cluster (8/81).

APPENDIX A

Table of Network-Located Events

Table A1

yr/mo/dy	hr	mn	sec	lat ° '	lon ° '	depth km	Mb	gap °	dn km	RMS sec	ERH# km	ERZ# km
81/ 6/20	23	19	38.40	52n19.21	173w18.72	29.58	5.4	357	470	.55	31.61	31.61
81/ 6/21	0	13	26.59	53n 7.44	166w33.36	11.58	3.4	333	84	.13	1.41	1.78
81/ 6/21	3	4	22.23	53n51.59	163w49.02	90.59	3.4	348	150	.13	3.83	6.89
81/ 6/21	8	9	16.32	52n15.71	156w50.60	5.75	4.2	347	181	.11	2.83	31.61
81/ 6/21	22	57	52.63	52n37.64	165w37.23	14.52	3.8	344	138	.13	2.51	31.61
81/ 6/22	15	46	7.23	53n29.08	155w49.90	21.04	2.7	315	48	.09	0.80	1.52
81/ 6/22	16	30	52.93	53n34.92	165w 2.85	18.24	3.7	335	78	.21	3.10	31.61
81/ 6/25	1	36	30.70	55n 1.45	158w48.92!	125.03	5.0	357	478	.63	31.61	31.61
81/ 5/26	8	6	25.47	53n40.44	166w47.51	34.26	2.5	294	27	.04	0.57	2.30
81/ 6/27	20	28	34.82	53n23.49	163w16.00	9.74	4.5	350	197	.11	3.76	31.61
81/ 6/27	22	59	45.40	53n23.69	163w 6.44	25.04	4.5	351	207	.15	4.30	31.61
81/ 6/28	0	47	38.43	52n24.17	166w50.87	25.00	3.8	345	166	.18	4.43	31.61
81/ 6/29	11	54	25.53	53n35.26	163w10.46	10.36	4.0	351	198	.58	14.39	31.61
81/ 7/ 1	9	10	0.57	53n51.67	164w27.56	52.09	3.6	343	109	.18	2.66	3.43
81/ 7/ 2	6	16	54.76	52n 4.65	165w39.23	14.78	3.9	346	199	.17	4.22	31.61
81/ 7/21	15	15	16.63	53n 1.47	167w57.03	74.79	3.1	345	117	.39	8.22	31.61
81/ 7/22	10	27	4.39	52n39.34	158w 0.82	25.02	3.8	347	152	.36	17.63	31.61
81/ 7/22	23	53	15.67	53n45.78	163w25.02	7.43	3.9	347	178	.42	9.92	31.61
81/ 7/27	2	41	12.96	53n 3.74	164w25.81	3.18	4.0	340	143	.15	2.42	31.61
81/ 7/27	10	27	45.21	53n33.30	166w38.61	81.42	3.4	302	24	.20	2.65	1.91
81/ 7/28	22	51	3.25	54n17.74	162w57.32	15.15	4.2	352	203	.20	8.47	31.61
81/ 7/31	2	14	8.70	53n59.34	167w 4.38	132.91	3.4	331	20	.18	5.06	31.61
81/ 7/31	2	31	27.94	54n 4.31	164w18.24	13.87	3.8	344	115	.38	6.44	31.61
81/ 8/ 1	18	46	17.40	52n37.22	167w 9.99	19.80	3.8	343	131	.18	3.52	31.61
81/ 8/ 2	6	40	23.11	52n39.78	169w14.071	20.31	4.3	352	209	.42	16.66	31.61
81/ 8/ 2	13	44	51.24	53n23.32	165w35.97	19.76	3.2	321	62	.15	0.92	0.84
81/ 8/ 3	8	32	36.41	53n21.79	165w36.25	5.45	3.5	321	64	.40	4.00	31.61
81/ 8/ 6	6	6	44.37	53n50.12	166w42.34	5.73	1.4	153	8	.04	0.17	0.90
81/ 8/ 6	14	59	35.65	53n50.22	166w42.02	4.60	2.4	149	8	.03	0.15	1.26
81/ 8/ 6	17	31	46.71	53n41.34	165w 1.95	34.08	4.1	329	76	.16	1.49	7.60
81/ 8/ 7	17	5	58.69	53n50.47	166w41.57	0.53	2.6	140	8	.09	0.25	0.54
81/ 8/ 7	17	6	10.07	53n48.49	166w37.26	3.79	1.8	161	7	.03	0.40	31.61
81/ 8/ 7	21	45	49.21	53n50.12	166w41.80	4.05	1.6	146	8	.02	0.15	31.61
81/ 8/ 7	21	46	31.41	53n50.16	156w42.10	3.75	2.1	150	8	.07	0.22	31.61
81/ 8/ 7	22	32	9.96	53n50.31	166w42.35	1.70	1.2	152	8	.06	0.19	0.31
81/ 8/ 8	21	44	32.63	53n50.07	166w41.93	5.40	1.8	150	8	.06	0.21	1.17
81/ 8/ 8	21	44	53.97	53n50.25	165w40.79	12.12	1.8	132	8	.26	0.91	2.35
81/ 8/ 8	22	55	26.54	53n50.11	166w41.70	3.63	1.6	144	8	.03	0.15	0.83
81/ 8/ 8	23	10	17.60	53n49.62	166w41.22	7.10	1.6	140	7	.08	0.30	1.08
81/ 8/ 9	19	54	35.83	51n39.03	171w50.60	35.50	5.0	356	419	.52	31.61	31.61
81/ 8/10	22	55	11.11	51n41.38	169w41.49	21.51	4.5	354	306	.08	31.61	31.61
81/ 8/11	8	45	27.70	53n49.96	165w41.36	7.54	1.6	140	7	.08	0.23	0.93
81/ 8/11	9	4	2.48	53n50.29	165w42.03	3.86	1.4	149	8	.09	0.23	31.61
81/ 8/11	9	26	27.30	53n50.23	166w41.89	2.14	1.5	147	8	.04	0.13	0.73
82/ 2/ 6	11	30	6.42	53n45.02	165w58.44	10.30	2.8	280	15	.04	0.43	1.27
82/ 2/ 7	6	7	17.16	51n44.92	176w50.401	59.98	6.1	357	719	.23	31.61	31.61
82/ 2/ 9	9	46	9.92	52n33.58	167w43.13	10.54	3.5	350	151	.07	2.85	31.61
82/ 2/ 9	13	10	55.23	53n 8.75	165w44.55	12.95	3.6	336	69	.08	0.90	1.15
82/ 2/10	4	41	59.44	53n54.75	165w55.54	17.08	2.0	262	17	.26	1.85	2.18
82/ 2/10	6	55	43.45	53n33.42	166w 4.29	31.03	3.0	300	32	.05	0.56	1.00
82/ 2/11	12	41	47.60	53n31.46	165w17.92	11.84	2.6	324	28	.07	0.83	31.61
82/ 2/11	20	16	43.02	53n43.57	165w59.15	84.42	3.4	282	17	.16	2.02	1.41
82/ 2/15	13	59	30.18	53n49.50	167w13.33	145.47	3.7	325	35	.09	2.07	1.26
82/ 2/16	5	23	49.49	53n18.52	166w44.90	57.60	2.9	330	51	.27	3.31	8.80
82/ 2/17	22	31	53.61	51n37.19	177w47.821	64.73	5.8	358	785	.57	31.61	31.61
82/ 2/19	2	50	56.94	53n49.95	164w28.051	5.40	4.6*	340	129	.18	2.40	3.35
82/ 2/19	3	43	33.46	53n52.15	164w29.28	5.88	3.6	340	107	.13	2.19	2.30
82/ 2/19	4	34	38.32	53n42.51	165w53.37	87.27	3.5	290	23	.29	3.75	3.95
82/ 2/19	11	41	35.84	52n 8.12	169w37.22	12.24	4.3	356	267	.42	31.61	31.61
82/ 3/15	14	53	15.55	52n42.52	152w32.731	3.99	4.5	349	271	.12	3.79	31.61
82/ 3/15	15	3	33.30	53n49.69	165w29.50	4.15	1.8	153	9	.12	0.50	31.61

yr/mo/dy	hr	mn	sec	lat ° '	lon ° '	depth km	Mb	gap °	dn km	RMS sec	ERH# km	ERZ# km
80/ 7/17	Ø	6	59.Ø3	53n34.81	165w48.13	14.17	2.5	306	37	.28	2.59	14.9Ø
80/ 7/17	6	5Ø	17.56	53n35.39	165w56.85	13.88	2.9	333	37	.15	1.72	31.61
80/ 7/18	11	37	45.22	53n33.49	156w53.17	14.68	2.7	312	4Ø	.34	2.81	31.61
80/ 7/19	2Ø	49	35.56	53n15.62	157w 2.57	11.31	3.5	33Ø	74	.24	2.5Ø	2.35
80/ 7/2Ø	12	23	23.53	53n25.77	167w19.31	5.42	2.9	334	64	.17	2.11	31.61
80/ 7/2Ø	23	23	9.52	53n[illegible]	161w33.38	94.44	3.8	343	1Ø5	.61	11.41	32.32
80/ 7/2Ø	23	36	15.27	54n26.2[illegible]	164w 1.17	15.Ø5	3.4	352	149	.32	2.85	31.61
80/ 7/24	1	33	16.17	53n27.91	166w51.27	1Ø.38	2.4	317	5Ø	.31	3.61	31.61
80/ 7/24	2	49	7.Ø3	53n35.13	165w2Ø.73	44.27	3.3	328	6Ø	.16	1.64	2.66
80/ 7/24	3	1	5.76	53n29.35	167w29.7Ø	25.2Ø	2.8	338	66	.Ø8	1.45	31.61
80/ 7/24	4	38	2Ø.23	53n31.53	167w28.39	37.95	2.9	338	52	.23	2.26	1.59
80/ 7/24	6	14	31.43	53n12.53	164w14.Ø1	1Ø.88	3.1	344	145	.4Ø	6.72	31.61
80/ 7/24	8	57	48.15	53n17.75	161w3Ø.4Ø	11.19	4.1	342	125	.46	9.Ø1	31.61
80/ 7/24	9	4	45.Ø3	53n11.57	164w 8.15	9.16	4.1	345	152	.21	3.82	31.61
80/ 7/24	1Ø	6	41.86	53n 8.21	166w35.81	5.76	3.Ø	332	83	.14	1.27	31.61
80/ 7/24	13	54	45.17	53n17.23	166w1Ø.87	5.4Ø	3.4	345	144	.33	5.95	31.61
80/ 7/3Ø	5	51	28.72	53n13.97	165w 7.11	43.25	3.4	334	69	.18	1.91	4.Ø8
80/ 7/3Ø	15	27	35.31	53n22.45	167w28.78	9.53	3.2	338	75	.23	2.97	3.67
80/ 7/3Ø	23	57	17.69	53n16.Ø7	166w58.Ø1	9.73	2.5	329	73	.23	1.75	31.61
80/ 7/31	5	13	41.33	53n32.47	166w3Ø.74	8.3Ø	2.2	312	42	.25	1.56	31.61
80/ 7/31	8	4Ø	58.Ø2	53n33.28	166w45.23	4.26	2.3	3Ø6	4Ø	.14	Ø.94	1.31
80/ 7/31	9	31	47.74	53n32.57	166w47.Ø6	5.66	1.9	3Ø9	41	.11	Ø.75	2.25
80/ 7/31	1Ø	56	Ø.9Ø	53n25.31	157w11.95	6.26	3.1	33Ø	6Ø	.32	2.72	31.61
80/ 7/31	12	49	56.25	52n35.97	167w21.2Ø	1Ø.69	3.8	344	151	.15	2.61	31.61
80/ 8/ 1	13	23	39.12	53n3Ø.72	151w55.93	21.59	3.9	353	28Ø	.41	15.Ø2	31.61
80/ 8/ 7	15	26	22.38	53n2Ø.63	167w3Ø.72	3.72	3.7	338	79	.32	4.92	5.33
80/ 8/ 9	6	33	59.27	53n32.36	166w47.53	4.76	2.8	3Ø9	42	.Ø7	Ø.57	Ø.64
80/ 8/19	2Ø	41	17.92	53n29.8Ø	166w48.12	5.85	2.8	313	46	.19	1.37	3.9Ø
80/ 8/19	2Ø	49	41.35	53n31.7Ø	166w48.18	5.Ø2	2.9	31Ø	43	.1Ø	Ø.89	Ø.87
80/ 8/23	11	38	58.33	53n17.53	166w 8.39	1Ø.Ø8	3.5	326	61	.26	2.Ø5	31.61
80/ 8/27	16	6	46.22	53n39.21	166w35.38	52.75	3.Ø	283	27	.15	1.71	1.71
80/ 8/28	7	19	22.93	53n29.93	165w47.59	13.Ø7	2.7	312	46	.13	Ø.94	Ø.61
80/ 8/3Ø	21	58	11.43	53n33.53	166w47.79	5.84	2.6	311	45	.Ø9	Ø.82	1.37
80/ 9/ 3	2Ø	1Ø	58.75	53n2Ø.72	165w19.Ø2	5.Ø9	2.9	323	63	.19	1.83	31.61
80/ 9/ 4	21	26	33.46	53n55.53	166w32.26	17.1Ø	2.1	147	3	.22	1.Ø8	1.15
80/ 9/ 9	15	52	39.92	53n13.25	165w25.45	38.32	3.4	329	71	.24	2.55	1.46
80/ 9/15	21	56	4.5Ø	53n31.36	156w27.81	18.82	3.5	3Ø5	4Ø	.17	1.58	7.38
80/ 9/19	18	27	27.14	53n37.Ø3	166w23.35	14.12	2.7	291	29	.23	2.37	6.25
80/ 9/21	17	3	53.73	51n59.55	17Øw Ø.27!	29.98	5.3	354	3Ø3	.97	31.61	31.61
80/ 9/21	17	13	9.Ø1	5Øn32.33	172w 1.79!	13.12	5.1	355	518	.53	31.61	31.61
80/1Ø/ 1	11	3Ø	27.62	51n33.57	165w53.Ø7	5.Ø6	2.7	319	73	.88	6.92	31.61
80/1Ø/ 5	3	18	45.93	53n29.35	155w48.7Ø	14.97	2.9	313	47	.25	2.1Ø	31.61
80/1Ø/ 5	4	27	51.2Ø	53n33.51	165w48.55	1.75	2.9	312	45	.17	1.Ø7	4.3Ø
80/1Ø/ 7	5	29	54.39	53n42.23	165w44.46	23.Ø2	4.Ø	313	31	.23	2.58	4.45
80/1Ø/ 9	9	16	19.79	53n29.78	166w46.97	3.45	2.8	313	46	.Ø8	Ø.54	1.71
80/1Ø/1Ø	21	21	2.76	53n24.64	165w53.63	8.82	2.8	321	51	.33	2.Ø3	31.61
80/1Ø/14	15	53	37.Ø9	53n38.19	165w38.17!	67.78	4.Ø	32Ø	41	.23	2.48	4.32
80/1Ø/15	8	Ø	55.34	53n3Ø.27	165w51.35	15.ØØ	2.6	314	46	.19	1.33	31.61
80/11/21	14	55	17.49	51n49.99	176w1Ø.Ø6!	52.98	5.6*	358	671	.52	31.61	31.61
80/11/23	6	37	19.39	53n35.8Ø	154w27.67!	33.41	3.1	343	115	.18	3.53	31.61
80/11/29	14	52	21.56	54n15.34	153w58.3Ø	29.49	3.1	348	137	.31	1Ø.Ø7	31.61
80/12/ 9	5	12	56.91	53n25.19	165w31.ØØ	25.69	3.Ø	328	53	.Ø9	1.24	31.61
80/12/13	19	33	42.28	53n28.99	165w49.Ø6	42.ØØ	3.5	319	45	.13	1.26	2.75
80/12/15	16	13	58.Ø2	53n34.29	166w19.49	1.8Ø	3.2	3Ø7	38	.17	1.Ø4	3.13
80/12/16	3	Ø	54.57	54n55.12	163w53.56	152.25	5.2	351	165	.24	6.91	31.61
81/ 6/17	9	27	19.11	53n53.21	165w 3.91	79.Ø7	3.3	333	68	.24	3.Ø1	4.Ø6
81/ 6/18	22	54	7.27	52n53.2[illegible]	161w55.12	5.94	4.6	352	297	.26	8.1Ø	31.61
81/ 6/19	18	32	12.21	53n23.2[illegible]	165w12.51	39.37	4.1	334	84	.19	3.2Ø	8.18
81/ 6/2Ø	6	2	1Ø.27	54n15.13	165w32.56	35.12	2.5	271	34	.25	1.65	4.27
81/ 6/2Ø	12	1Ø	12.55	54n 9.35	161w 5.12	111.55	3.5	347	128	.Ø8	2.55	2.16
81/ 6/2Ø	15	46	14.34	53n25.12	156w13.23	13.ØØ	2.4	317	53	.Ø9	Ø.74	31.61

yr/mo/dy	hr	mn	sec	lat ° '	lon ° '	depth km	Mb	gap d	dn km	RMS sec	ERH# km	ERZ# km
82/ 3/19	19	30	40.05	53n41.50	166w17.69	93.56	3.7	237	14	.20	1.99	1.26
82/ 3/24	0	15	12.93	53n49.20	166w14.23	91.16	3.0	190	6	.09	1.06	0.74
82/ 3/24	22	0	7.92	53n51.07	164w41.15	29.81	3.2	337	95	.14	1.31	31.61
82/ 3/25	12	15	43.07	53n24.21	165w 3.05	20.11	3.6	330	87	.12	1.63	31.61
82/ 3/29	1	20	6.04	53n12.90	166w10.28	40.74	2.6	331	69	.11	1.61	7.06
82/ 3/30	6	13	13.56	53n44.29	167w30.45	41.88	3.0	339	53	.25	5.91	4.72
82/ 3/30	22	21	58.81	53n33.15	166w44.65	8.91	2.2	317	24	.10	0.70	0.30
82/ 4/ 2	11	17	21.80	53n30.52	165w56.99	55.61	3.2	307	39	.19	2.82	4.61
82/ 4/ 4	23	40	7.20	52n50.95	171w35.29l	16.98	4.6	357	341	.13	31.61	31.61
82/ 4/11	0	22	5.60	53n 5.11	166w32.50	5.96	3.3	336	76	.18	1.99	31.61
82/ 4/14	3	6	1.50	54n21.38	163w 0.80	19.84	4.0	352	200	.31	12.04	31.61
82/ 4/15	16	21	13.06	54n13.59	161w31.91l	150.45	5.3*	354	295	.45	31.61	31.61
82/ 4/16	8	46	55.88	53n18.55	163w 5.92l	25.00	3.9	347	210	.40	10.95	31.61
82/ 4/22	0	40	34.26	53n17.65	166w18.02	61.19	3.1	325	59	.31	3.35	7.01
82/ 4/24	0	32	20.86	53n55.41	166w36.81	0.52	1.7	269	6	.30	1.58	1.16
82/ 4/28	16	54	33.70	53n 4.05	166w40.88	34.87	3.8	338	78	.24	2.84	31.61
82/ 5/ 2	11	13	14.62	53n26.53	165w 0.80	12.28	3.4	331	87	.06	0.65	0.81
82/ 5/ 2	17	57	9.69	53n10.35	170w34.67l	23.58	4.5	358	265	.25	31.61	31.61
82/ 5/ 8	8	10	10.93	53n29.56	164w47.46	2.70	3.4	333	98	.25	3.34	31.61
82/ 5/10	3	17	29.97	51n25.96	170w22.44	49.90	4.4	357	359	.70	31.61	31.61
82/ 5/10	14	37	14.30	53n28.17	164w10.66	10.50	3.7	341	137	.30	6.30	31.61
82/ 5/14	9	28	57.23	53n43.59	167w14.35	10.50	2.8	345	36	.04	1.10	31.61
82/ 5/14	18	24	38.13	53n43.73	167w14.42	10.51	2.8	344	36	.06	1.25	31.61
82/ 6/ 3	5	55	13.05	52n22.90	166w12.40	8.85	3.7	348	157	.40	19.04	31.61
82/ 6/ 3	17	24	9.69	52n 5.76	163w45.06l	8.50	4.8	355	231	.95	31.61	31.61
82/ 6/ 4	12	50	18.59	52n 6.65	168w52.54l	27.09	4.0	355	235	.04	31.61	31.61
82/ 6/ 4	17	3	30.96	52n47.87	167w29.61	15.45	3.9	349	120	.06	2.03	31.61
82/ 6/ 5	21	11	11.85	53n27.35	165w10.04	10.81	3.2	327	78	.21	2.29	31.61
82/ 6/ 6	1	13	58.22	52n22.25	169w15.33	54.89	4.4	355	231	.28	31.61	31.61
82/ 6/ 6	5	7	24.46	52n24.22	166w42.82l	25.08	4.2	347	152	.12	4.65	31.61
82/ 6/ 7	4	49	33.18	52n34.35	166w14.05	4.81	3.8	344	136	.07	1.77	31.61
82/ 6/ 8	17	29	59.59	53n25.20	164w53.74	25.01	3.4	332	95	.09	1.14	31.61
82/ 6/ 8	17	47	26.83	53n25.32	164w58.72	15.27	3.2	331	90	.21	1.45	0.96

\# ERH and ERZ default to a value of 31.61.
l Event also located by PDE
* Magnitude as given in PDE

Appendix B

Focal Mechanism for the Nateekin River Seismic Cluster

Earthquake source mechanisms are commonly derived from P-wave first motion data from a single event. Assuming that the source process can be represented by a double-couple force system it is possible to define two orthogonal planes along which rupture may have occurred. To constrain which plane is the actual rupture plane further evidence, either seismic or geologic must be used. If a group of earthquakes are spatially related and it is believed that they all represent rupture along a single fault plane, a composite source mechanism can be obtained by using first motion data from the group.

The focal mechanism for the Nateekin Seismic Cluster is shown in Figure B1 on an upper-hemisphere, equal-area, stereographic projection. The possible rupture planes separate quadrants of compessional an dilatational first motion. The position of each first motion is controlled by the take-off angle of the seismic ray travelling from the source to the station and the azimuth of the station with respect to the source.

First motions for ten of the thirteen located events were used in this composite focal mechanism. The remaining three events had poorly controlled depth estimates, thereby producing poorly constrained takeoff angle estimates. Figure B2 shows the log of the P to SV amplitude ratio for all of the observed arrivals which showed a clear P-wave and an unclipped S-wave. This ratio should be small near the nodal planes and large near the P and T axes. There is good qualitative agreement between the nodal planes defined from the P-wave first motions and the observed P to SV amplitude ratios.

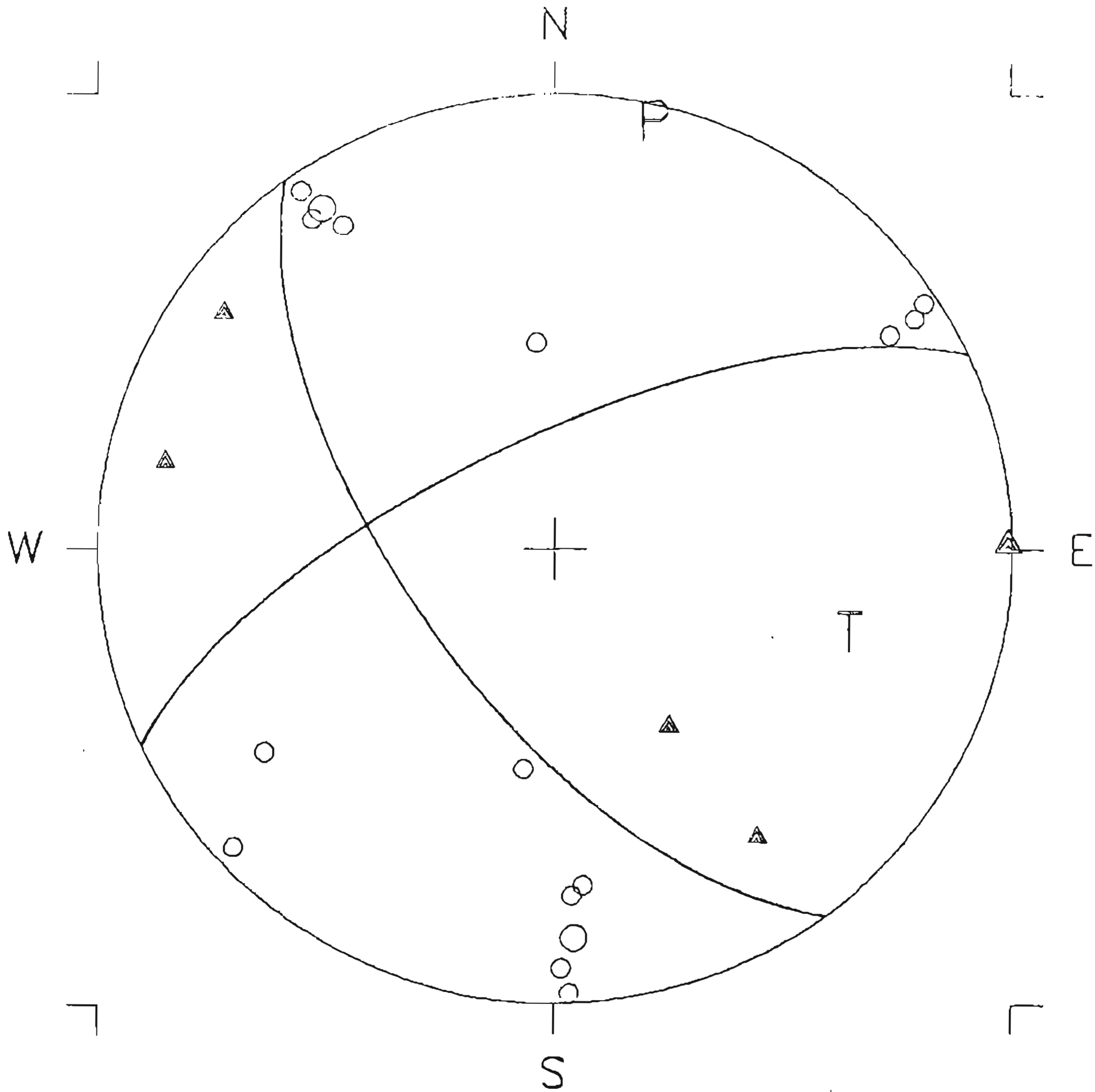

Comp. 8–81 p=13–4 t=106–34 b=277–56
Equal Area Upper Hemisphere
△ =impulsive compression, ○ =impulsive dilatation
▲ =emergent compression, ○=emergent dilatation,

Figure B1. Composite first motion plot of events forming the Naceekin River sequence.

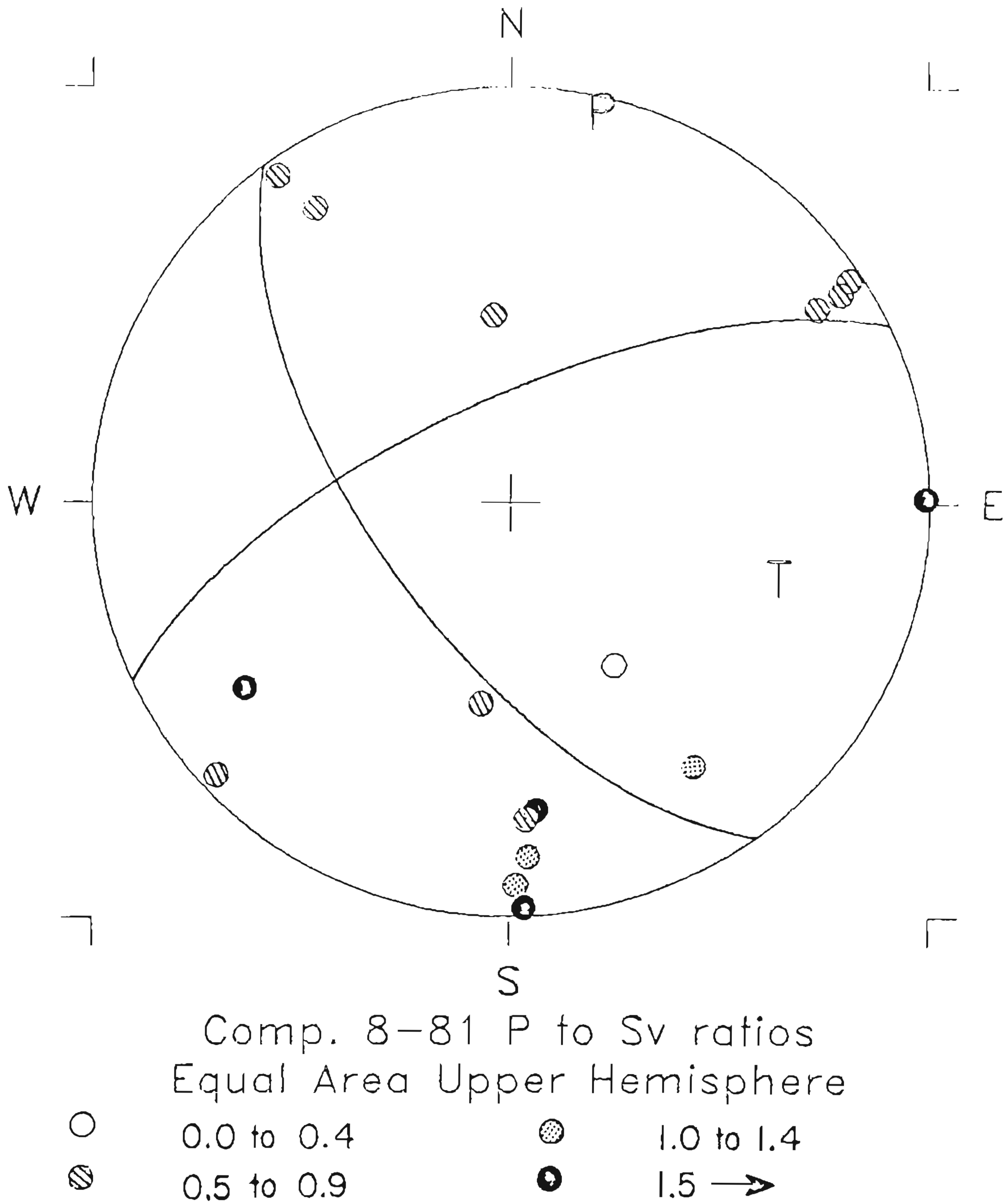

Figure 82. Plot of the relationship between the implied fault plane solution from first motion data, and log P-to-SV amplitude ratios.

Appendix C

Network Statistics

Usable local earthquake data became available from Unalaska Island in 1980 with the installaton of the local five-station seismic network. Due to the extreme aleutian weather and restricted yearly field maintenance, significant observational gaps occurred during the lifetime of the Unalaska array (Figure C1). Due to this significant amount of down time, the actual number of events observed during the two and a half year operational lifetime of the network is roughly equivalent to that occurring during a single year.

During the operational lifetime of the network the rate of local seismicity varied from zero events per day to over ten per day during the Nateekin swarm (Figure C1). The bulk of the seismicity observed, however, occurred at distances between 40 and 400 km (Figure C1 S-P=5-50 sec). The maximum number of events observed per-day in this distance range was 32, on March 24, 1980. These events were aftershocks to an M_s=6.2 earthquake located at 52.969N, 167.670°W.

The rate and magnitude distribution of the seismicity observed by the local network can be compared with that observed by the world-wide standardized seimic network (WWSSN) using frequency and cumulative seismicity plots (Figure C2). Magnitude bounds overwhich the cumulative seismicity decreases linearly indicates levels of complete recording (i.e., the minimum magnitude of bound, referred to as the minimum magnitude of completeness, is the magnitude above which all events that occur are recorded). The lower limit of complete recording for the WWSSN in the Unalaska region is M_b = 5.0 (Habermann, 1981; FigureC2-A). The lower limit of complete recording of events around Unalaska (Distances < $\approx$ 75 km) is about M_b = 3.2 (Figure C2-B). For the Nateekin swarm, events down to M_b = 1.0 were detected, but complete recording of this activity probably extends down to M_b = 1.2 or 1.4. From these estimates of the level of complete recording it can be seen that the installation of the local seismic network has reduced the level of completeness, within the restricted area of the network, by a fator of about 3.5 over that achieved by the WWSSN.

Also included on Figure C2 are estimates of the slope of the linear portion of the cumulative magnitude-frequency distribution. These estimates are commonly referred to as B-values and describe the rate of occurrence of the different magnitude events. The B-value for the events observed by the WWSSN is 1.12 $\pm$ 0.09 while that observed by the local array is 0.60 $\pm$ 0.13. The B-value derived from the local data appears to be significantly less than that derived from the WWSSN. This difference, however, may not be significant due to the relatively few earthquakes observed by the local network. This lack of data manifests itself in the "ragged" appearance in the magnitude-frequency distribution. If it is representative of the local seismicity, however, the differences in B-values obtained by the two networks may be interpreted as indicating that the dominant mode of stress release due to seismic processes during the interseismic period occurs as events with magitudes between 4.6 and 5.8.

Figure C1. Number of earthquakes recorded per day by the Unalaska Seismic array in 1980, 1981, and 1982. Data are grouped according to S-P travel time.

DUTCH HARBOR EVENT COUNT 1980

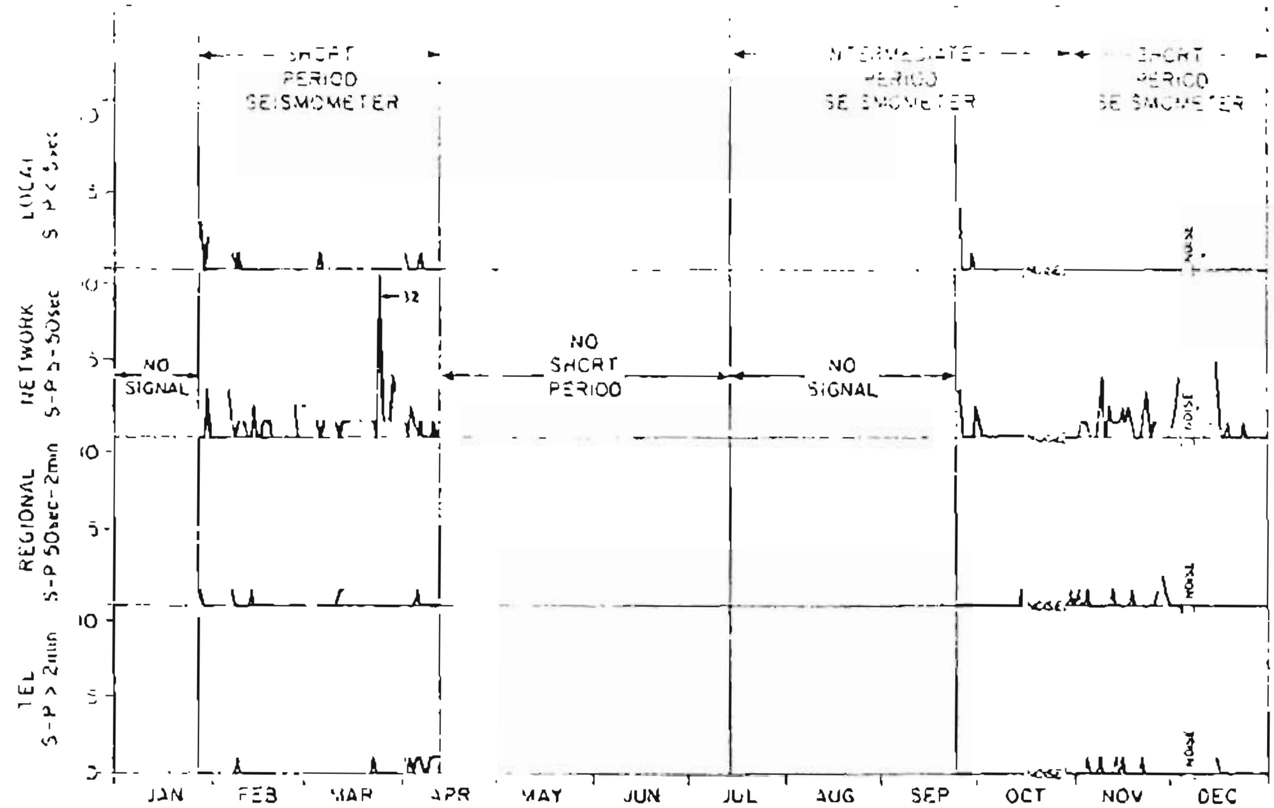

DUTCH HARBOR EVENT COUNT 1981

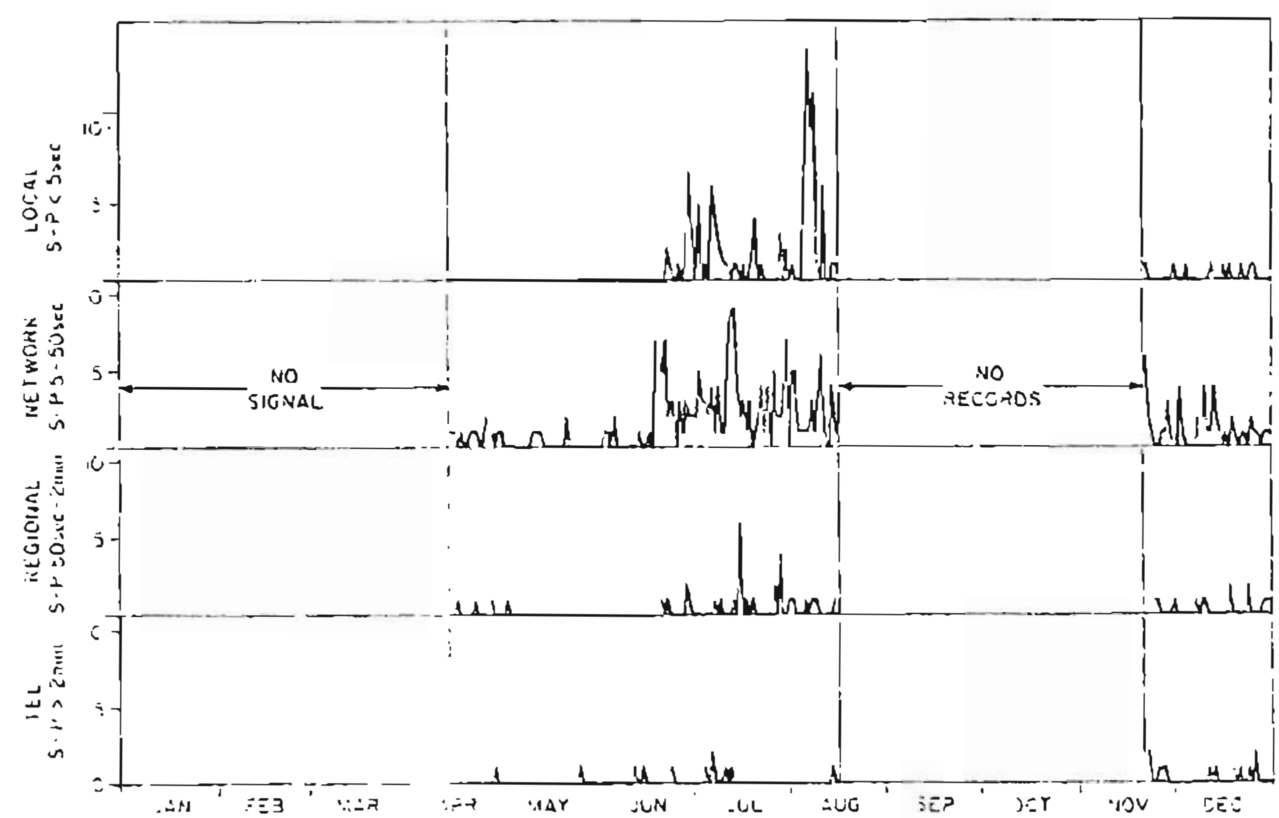

DUTCH HARBOR EVENT COUNT 1982

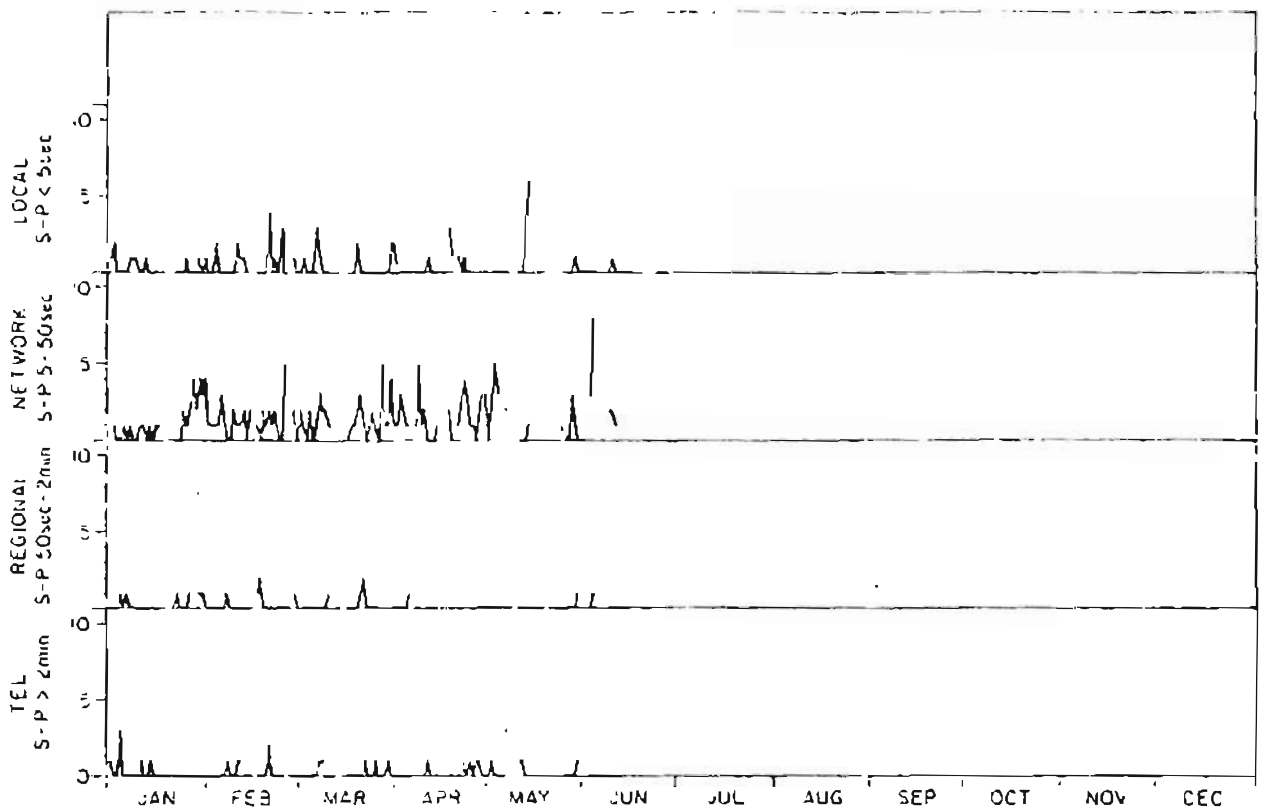

Figure C2. Magnitude frequency relationships for; A) earthquakes recorded by the WWSSN originating between 172°W-158°W, B) earthquakes recorded by the Unalaska array, C) all observed events from the Nateekin sequence. Solid lines represent the number of events occurring within each magnitude interval while dashed line, indicate the cumulative number of events observed. Best fit, maximum likelyhood estimates of the slope of the linear portion are also included as an estimate of the B-value.

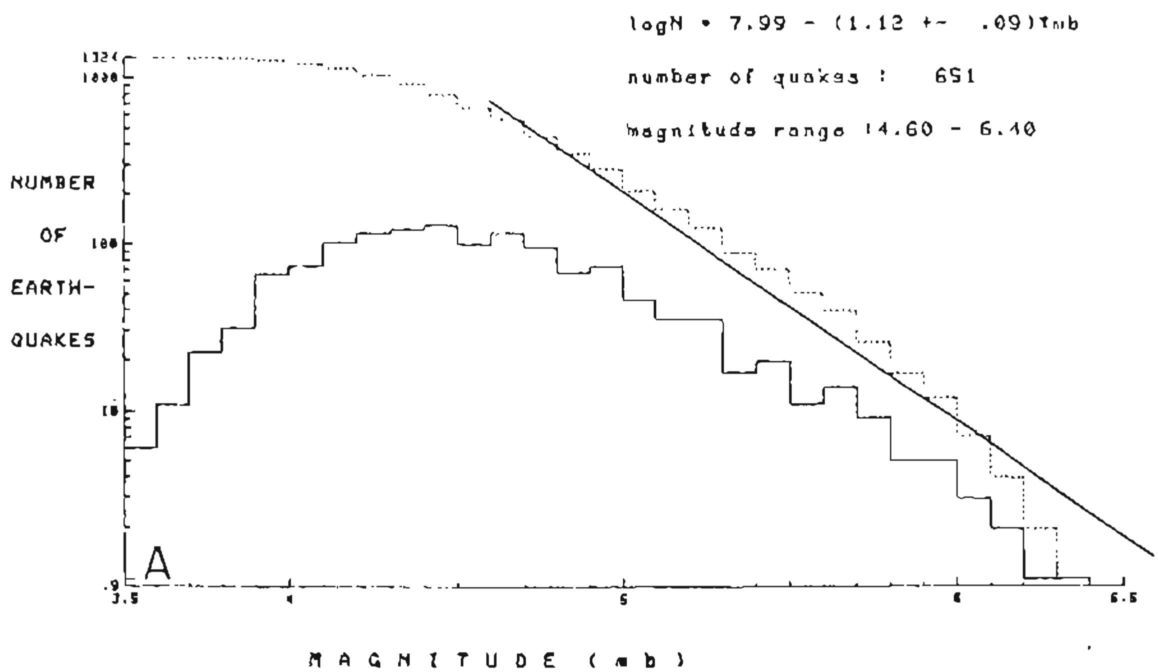
logN = 7.99 - (1.12 +- .09)*mb
number of quakes : 651
magnitude range : 4.60 - 6.40
NUMBER
OF
EARTH-
QUAKES
1000
100
10
.9
A
3.5
4
5
6
6.5
M A G N I T U D E (m b)

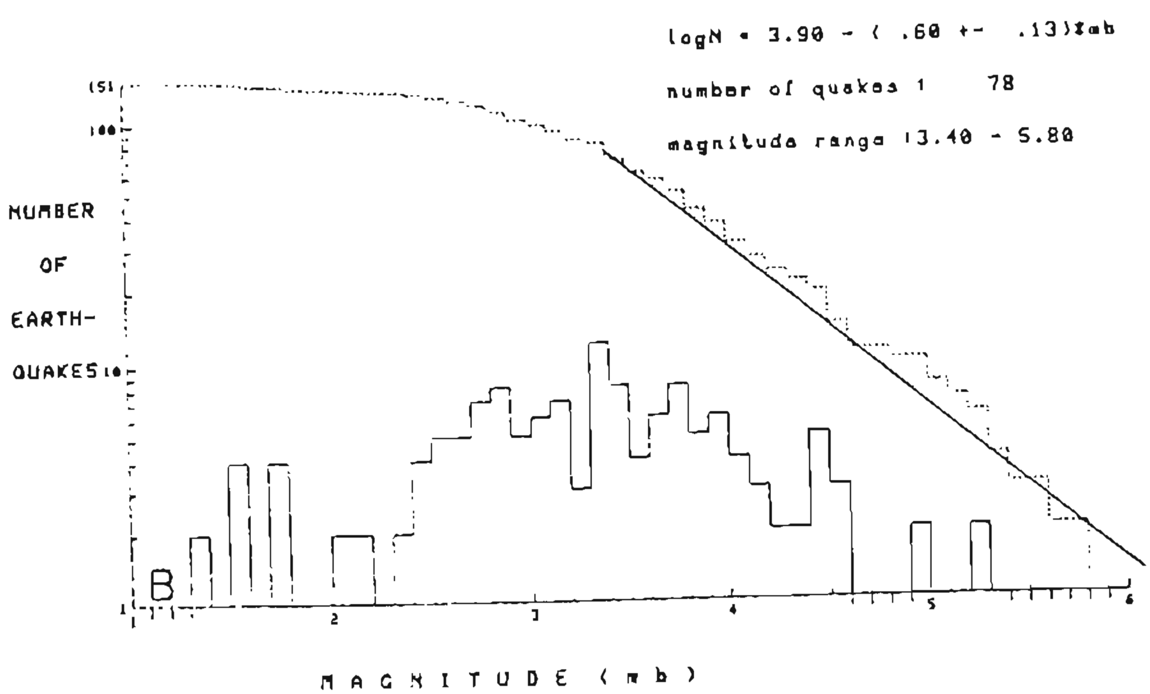
logN = 3.90 - (.60 +- .13)*mb
number of quakes : 78
magnitude range : 3.40 - 5.80
NUMBER
OF
EARTH-
QUAKES
100
10
1
B
2
3
4
5
6
M A G N I T U D E (m b)

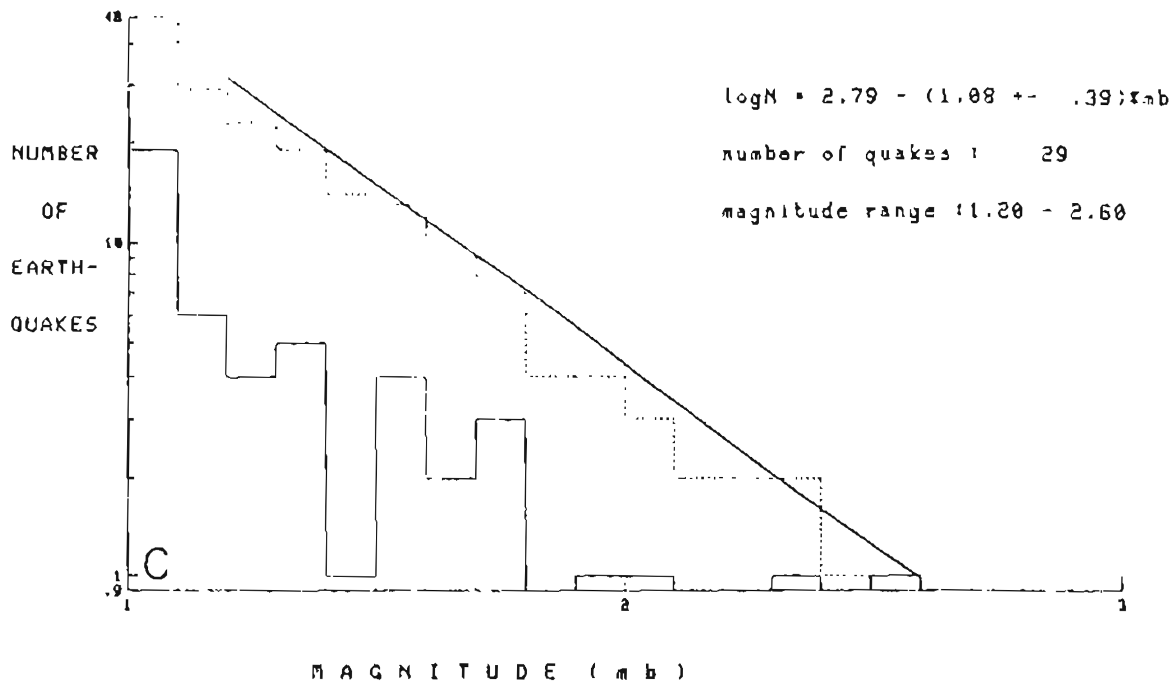
logN = 2.79 - (1.08 +- .39)*mb
number of quakes : 29
magnitude range :1.20 - 2.60
NUMBER OF EARTH-QUAKES
10
1
.9
C
1
2
3
MAGNITUDE (mb)